

Comments to the Author:

The authors have responded most of the referee comments. However, when looking at the revised paper, there are still a few issues that should be considered before accepting this paper for publication. They are listed below.

We thank the editor for carefully reviewing the manuscript, and all the comments have been addressed.

In the introduction the authors discuss marine aerosols in very general terms, but then mention emission trends that are not true in general in the global atmosphere (lines 97-100). Please either mention explicitly here that you refer to Asian emissions, or revise the text according to what has taken place in different continents (In Europe and NA, for example, SO₂ emissions have decreased for several decades and also NO_x emissions have evolved very differently from those in Asia).

Response: The emission trend is mainly applied to China, and this has been added in the revised manuscript.

line 161: Surface tension is a composition-dependent variable, not a constant. It is usually set constant when applying the equation to calculate the hygroscopicity parameter κ , but that is a different thing. Please correct the text.

Response: This has been revised as follows:

$\sigma_{s/a}$ represents the surface tension over the interface of the solution and air with the value of 0.072 J m⁻² applied in this study

Lines 362-369: The minimum diameter of particles at SS of 0.2-1 % is somewhere in the range 50-100 nm, so statement about nanometer-size particles on lines 366-367 is very confusing. Why to talk about nanometer-size (sub-10 nm) particles here? Is this statement even correct? There is often more organics in sub-100 nm particle compared with accumulation mode particles, but the situation in the sub-10 nm size range may be totally different. Please be more careful here what size ranges you are really referring to here.

Response: This has been revised as follows:

In general, the fraction of organics in the nanometer particles increases with decreasing particle size from ~100 nm to ~50 nm

Section 3.6, end of Introduction and Figure 7: I would recommend using the terms "relationship" or "regression equation" rather than "correlation" here. The term "correlation equation" does not sound correct at all.

Response: This has been revised based on the reviewer's suggestion.

The text still contains many grammatical problems (lack of articles, wrong prepositions etc.). Please check out the text once more with the help of a native English speaker.

Response: We have asked a native speaker to check the grammar issues.

1 **Variations in N_{cn} and N_{ecn} over ~~China~~-marginal seas in China related to marine**
2 **traffic emissions, new particle formation and aerosol aging–**

3 Yang Gao^{1,2#*}, Deqiang Zhang^{1#}, Juntao Wang¹, Huiwang Gao^{1,2} and Xiaohong Yao^{1,2*}

4 ¹Frontiers Science Center for Deep Ocean Multispheres and Earth System, and Key Laboratory
5 of Marine Environment and Ecology, Ministry of Education, Ocean University of China,
6 Qingdao, 266100, China

7 ²Laboratory for Marine Ecology and Environmental Science, Qingdao National Laboratory for
8 Marine Science and Technology, Qingdao, 266237, China

9 #Authors contribute equally to this study

10 *Correspondence to yanggao@ouc.edu.cn; xhyao@ouc.edu.cn

Style Definition: Comment Text: Font: (Default) Tahoma, 8 pt

Style Definition: Comment Reference: Font: (Default) Tahoma, 8 pt

Formatted: Font: +Body (Calibri), 10.5 pt

Formatted: Normal

34
35
36
37
38
39
40
41
42
43
44
45
46
47
48
49
50
51
52
53
54
55
56
57
58
59
60
61
62
63
64
65
66

Abstract

Formatted: Centered

In this study, a cruise campaign was conducted over ~~China~~-marginal seas in China to measure the concentrations of condensation nuclei (N_{cn}), cloud condensation nuclei (N_{ccn}) and other pollutants ~~during-from day of year (DOY)~~ 110 to DOY 135 of 2018. ~~With exhaustedly excluded-The ship self-ship~~ emission signals, ~~were exhaustively excluded, and~~ the mean values of N_{cn} during the cruise campaign were found to slightly ~~increased~~increase from $3.2 \pm 1.1 \times 10^3 \text{ cm}^{-3}$ (mean \pm standard) at supersaturation (SS) of 0.2% to $3.9 \pm 1.4 \times 10^3 \text{ cm}^{-3}$ at SS of 1.0%, and the mean value for N_{cn} was $8.1 \pm 4.4 \times 10^3 \text{ cm}^{-3}$. Data analysis showed that marine traffic emissions apparently ~~yielded a large contribution~~largely contributed to the increase ~~of~~in N_{cn} in the daytime, especially in the marine atmospheres over ~~their~~ heavily ~~travelled~~traveled sea zones; however, the fresh sources ~~had made~~ no clear contribution to the increase ~~of~~in N_{ccn} . This finding was supported by the quantitative relations between N_{cn} and N_{ccn} at SS=0.2-1.0% against the mixing ratios of SO_2 in the ship self-ship emission plumes, i.e., a 1 ppb increase in SO_2 ~~corresponds~~corresponded to a $1.4 \times 10^4 \text{ cm}^{-3}$ increase in N_{cn} , but only a 30-170 cm^{-3} increase in N_{ccn} , possibly because of abundant organics in the aerosols. ~~The smooth~~Smooth growth ~~of~~can be observed in the marine traffic-derived particles ~~can be observed~~, reflecting aerosol aging. The estimated hygroscopicity parameter (κ) values were generally as high as 0.46-0.55 under the dominant onshore winds, suggesting that inorganic ammonium aerosols likely ~~acting~~acted as the major contributor to N_{ccn} largely through aerosol aging processes ~~largely decomposed of decomposing~~ organics. Moreover, the influences of the new transported ~~new~~ particles from the continent on the N_{cn} and N_{ccn} in the marine atmosphere were ~~also~~ investigated.

Key wordsKeywords: N_{cn} ; N_{ccn} ; marine traffic emissions; hygroscopicity parameter; SO_2

67
68
69
70
71
72
73
74
75
76
77
78
79
80
81
82
83
84
85
86
87
88
89
90
91
92
93
94
95
96
97
98
99

1. Introduction

Oceans occupy approximately 2/3 of the Earth's surface, and water evaporation from oceans acts as the major source of moisture in the atmosphere. Aerosol-cloud interactions in marine atmospheres, covering ranging from tropic to polar regions, thereby have attracted great attention in the past few decades due to their impact on the climate change (Huebert et al., 2003; Yu and Luo, 2009; Quinn and Bates, 2011; Wang et al., 2014; Brooks and Thornton, 2018; Rosenfeld et al., 2019). However, large uncertainties still exist in various marine atmospheres, e.g., the sources of aerosols, the concentrations of bulk cloud condensation nuclei (CCN) and aerosol CCN activation under various supersaturations. (Clarke et al., 2006; Decesari et al., 2011; Quinn and Bates, 2011; Saliba et al., 2019; Rosenfeld et al., 2019). These uncertainties are mainly determined by limited observations in marine atmospheres, although a few additional observations of the number concentrations of aerosols (N_{cn}) and CCN (N_{ccn}) were recently reported in different marine atmospheres, e.g., over the Mediterranean (Bougiatioti et al., 2009), Sea of Japan (Yamashita et al., 2011), Bay of Bengal (Ramana and Devi, 2016), coast of California (Ruehl et al., 2009) and the Northwest Pacific Ocean (Wang et al., 2019); etc.).

Besides in addition to sea-spray aerosols and secondarily formed aerosols from sea-derived gaseous precursors (O'Dowd et al., 1997; Clarke et al., 2006; Quinn and Bates, 2011; Blot et al., 2013; Fossum et al., 2018), marine traffic emits large amounts of aerosols and reactive gases (Chen et al., 2017). These pollutants may also directly or indirectly contribute to CCN therein, to some extent (Langley et al., 2010). In addition, the long-range transport of continental aerosols has

100 ~~been~~ widely ~~reportedly acted~~~~reported to act~~ as an important source of CCN in marine
101 atmospheres (Charlson et al., 1987; Huebert et al., 2003; Fu et al., 2017; Royalty et al.,
102 2017; Sato and Suzuki, 2019; Wang et al., 2019). The continent-derived aerosol
103 particles observed in marine atmospheres usually mix with different sources, such as
104 biomass burning, dust and anthropogenic emissions (Feng et al., 2017; Lin et al., 2015;
105 Guo et al., 2014; Guo et al., 2016). An appreciable fraction of organics reportedly exists
106 in marine aerosols and continental aerosols upwind of oceans (O'Dowd et al., 2004;
107 Feng et al., 2012; Quinn et al., 2015; Feng et al., 2016; Song et al., 2018; Ding et al.,
108 2019). However, ammonium sulfate aerosols have been frequently reported to
109 dominantly contribute to CCN-related aerosols in many marine atmospheres and lead
110 to hygroscopicity ~~parameter~~~~parameters~~ (κ) larger than 0.5 (Mochida et al., 2010; Cai et
111 al., 2017; Fu et al., 2017; Royalty et al., 2017; Phillips et al., 2018). A question is
112 ~~automatically~~~~naturally~~ raised, i.e., where do particulate organics go in the marine
113 aerosols enriched in ammonium sulfate? Anthropogenic ~~emission~~~~emissions in China~~
114 such as SO₂, ~~and~~ NO_x ~~in general increase~~~~have generally increased~~ since ~~the~~ 1980s, ~~until~~
115 ~~and~~ recently started to decrease, i.e., SO₂ ~~start~~~~started~~ to decrease ~~from~~~~in~~ 2006 (Li et al.,
116 2017), whereas NO_x started to decrease ~~since~~~~in~~ 2011 (Li et al., 2017; Liu et al., 2016).
117 Together with the influence of the Asian ~~Monsoon~~~~monsoon~~, the marginal seas of China
118 are, ~~therefore~~, inevitably affected by the outflow of continental aerosols (Guo et al.,
119 2016; Feng et al., 2017). Observations of N_{cn} and N_{ccn} in marine atmospheres over China
120 marginal seas ~~help~~~~help~~ to ~~resolve~~~~address~~ the data scarcity, understand ~~their~~~~the~~ sources
121 and dynamic changes ~~in these parameters~~ and ~~better service the study of~~ their potential
122 climate impacts.—

123

124 In this study, cruise campaigns were conducted to measure the N_{ccn}, N_{cn}, particle
125 number size distributions, gaseous pollutants and aerosol composition of water-soluble
126 ionic species over the marginal seas from 20 April 2018 (day of year (DOY) 110) to 15
127 May 2018 (DOY 135), traveling from the East China ~~sea~~~~Sea~~ to the South China ~~sea~~~~Sea~~
128 and returning to the Yellow ~~sea~~~~Sea~~. Spatiotemporal variations in ~~the~~ N_{cn}, N_{ccn} and CCN
129 activities of ~~the~~ aerosol particles were studied. The *Kappa* values of ~~the~~ aerosol particles

130 from DOY 110 to DOY 118 over the marine ~~environments~~ were calculated and analyzed.
131 Finally, we tried to establish ~~the correlations~~relationship of N_{cn} and N_{ccn} with ~~the~~ mixing
132 ratios of SO_2 in self-ship plumes and ambient marine air. The ~~correlation~~regression
133 equations are valuable for the estimation of N_{cn} and N_{ccn} from SO_2 when the direct
134 observations of N_{cn} and N_{ccn} are not available.

135

136 2. Experimental design

137 2.1 Instruments and data sources

138 A cruise campaign was conducted across ~~China~~-marginal seas ~~in China~~ from DOY 110
139 to DOY 135 of 2018 (Fig. 1a,b). A suite of instruments including a ~~Fast Mobility~~
140 ~~Particle Sizer~~fast mobility particle sizer (FMPS, TSI Model 3091), CCN counter
141 (CCNC, DMT Model 100), ~~Condensation Particle Counter~~condensation particle
142 counter (CPC, TSI Model 3775), gas analyzers, ~~Ambient Ion Monitor~~ion
143 ~~monitor-ion~~ chromatography (AIM-IC), etc., were onboard ~~at~~the commercial cargo
144 ship *Anqiang 87* for measurements. The FMPS was used to measure ~~the~~ particle number
145 size distributions with mobility diameters from 5.6 nm to 560 nm in 32 channels at 1-
146 second temporal resolution with an inlet flow of 10 L min^{-1} . The CPC was used to report
147 the N_{cn} ranging from 4 nm (50% efficiency) to 3000 nm (N_{cn}) in 2-second time
148 resolution with an inlet flow of 1.5 L min^{-1} . The N_{cn} was then used to calibrate the
149 particle number size distributions simultaneously measured by the FMPS, ~~on~~the basis
150 of the procedure proposed by Zimmerman et al. (2015). Due to the severe oceanic
151 ~~condition~~conditions and humid weather conditions, the FMPS and CPC were out of
152 service after DOY 118 and DOY 122, respectively. Prior to the campaign, the CCNC
153 was calibrated with ammonium sulfate particles based on the standard procedure
154 detailed ~~at~~by Rose et al. (2008). The calibration curve ~~was~~is shown in Fig. S1. The total
155 flow rate of CCNC was 0.45 L min^{-1} , with a ratio of sample to sheath at 1/10, and five
156 ~~super saturations~~supersaturations (SS) conditions were selected, including 0.2%, 0.4%,
157 0.6%, 0.8%, and 1.0%. More detailed information about the measurement of N_{ccn} can
158 be found in Wang et al. (2019).

159

160 During the experiment, ambient particles were first sampled through a conductive tube
161 (TSI, US) and a diffusion dryer filled with silica gel (TSI, US), and then ~~splitted~~
162 ~~into~~split for analysis by means of different instruments with a splitter. All instruments
163 were placed in an air-conditioned container on the deck of ~~the~~ ship, with ~~an~~ inlet height
164 of approximately 6 m above ~~the~~ sea level. Regarding the gas analyzers, the ambient O₃
165 (Model 49i, Thermo Environmental Instrument Inc., USA C-series), SO₂ (Model 43i,
166 Thermo Environmental Instrument Inc., USA C-series), and NO_x (Model 42i, Thermo
167 Environmental Instrument Inc., USA C-series) were measured in mixing ratios with ~~a~~
168 temporal resolution of one-~~_~~minute. The CCNC and gas analyzers were operated
169 properly throughout the entire campaign. The same was true for ~~the~~ AIM-IC, which was
170 used to measure ~~the~~ water-soluble ionic species in ~~the~~ ambient particles ~~less~~sized
171 ~~smaller~~ than 2.5 μm.

172

173 In this study, the ~~Hybrid Single Particle~~hybrid single-particle Lagrangian ~~Integrated~~
174 ~~Trajectory~~integrated trajectory (HYSPLIT) model from the NOAA Air Resources
175 Laboratory was used to track the particle sources. The input of HYSPLIT, such as wind
176 speed and wind direction, was ~~obtained~~ from the National Center for Environmental
177 Prediction (NCEP) Global Data Assimilation System (GDAS) with ~~a~~ spatial resolution
178 of 0.5 ~~degree-degrees~~.

179

180 The hygroscopicity parameter (κ) was calculated according to the method proposed by
181 Petters and Kreidenweis (2007).

182
$$\kappa = \frac{4A^3}{27D_d^3 \ln^2 S_c}, \quad A = \frac{4\sigma_{s/a} M_w}{RT\rho_w}$$

183 where D_d is the dry diameter, S_c is the ~~super saturation~~supersaturation, M_w is the
184 molecular weight of water, ~~σ_{s/a} a constant of 0.072 J m⁻²~~ represents the surface
185 tension over the interface of the solution and air ~~with the value of 0.072 J m⁻² applied~~
186 ~~in this study~~. R is the universal gas constant, T is the ambient temperature and ρ_w is
187 the water density. ~~The~~-D_d was not measured directly and ~~was~~ assumed to be equal to

Formatted: Font color: Black

Formatted: Not Highlight

Formatted: Not Highlight

188 the critical diameter for CCN activation (D_{crit}). D_{crit} was defined as the particle diameter
189 down to which ~~by integrating~~ from the largest diameter with the integrated number
190 concentration equal to the CCN concentration (Hung et al., 2014; Cheung et al.,
191 2020). The FMPS ~~has had~~ a low size resolution, particularly at the sizes greater than
192 90 nm, which ~~doesn't did not~~ allow accurate calculation of the
193 *Kappa* values at SS=0.2%. At SS=0.6% and 0.8%, the *Kappa* value was not calculated
194 considering the complication in the explanation of the value, possibly reflecting the
195 combined effects of particle size, mixing state and chemical composition.—

196

197 2.2 Separating ambient signals of N_{cn} and N_{ccn} from ship self-ship emission emissions

198 The data measured during the cruise campaign were frequently ~~interfered by~~ subject to
199 interference from self-ship emission signals. from the ship. The N_{cn} and N_{ccn} over the
200 marginal seas were first distinguished based on the source of the ambient environment
201 or the ship self-ship emission emissions. The data measured at 18:00-24:00 on DOY
202 115 ~~were~~ used to illustrate the separation (in Fig. 2), with, and the size distribution
203 of the particle number concentration during DOY DOYs 110-118 is shown in Fig. S2-
204 S10 in the supporting information. At 18:00-21:11 LT (~~Local Time~~, the local time), a
205 low N_{cn} of $5.8 \pm 0.4 \times 10^3 \text{ cm}^{-3}$ ~~were~~ was observed. The accumulation mode dominated
206 ~~in the~~ particle number concentration with ~~the~~ a median mobility mode diameter at
207 105 ± 4 nm (Fig. 2a). Afterwards, the N_{cn} rapidly increased by over one order of
208 magnitude (Fig. 2b). The dominant particle number concentration mode changed from
209 accumulation mode to Aitken mode, with the median mobility diameter of the Aitken
210 mode stabilized at $47 \pm 4 \text{ nm}$ ~~in for~~ for approximately 90% of the time. The rapid increase in
211 N_{cn} and the change in the mode size indicated the signal of the emissions of the ship
212 emission-itself. The ship self-ship emission interference after 21:11 was ~~also~~ supported
213 by additional evidence, e.g., a large decrease in the activation ratio (AR),
214 defined as the quotient of N_{ccn} and N_{cn} , from >0.5 to <0.2 at SS=0.4% (Fig. 2c) due to
215 a large increase ~~of in~~ in N_{cn} but a much smaller magnitude enhancement of N_{ccn} (Fig. 2b),
216 a rapid increase ~~of in~~ in NO_x from $<10 \text{ ppb}$ to $192 \pm 99 \text{ ppb}$, NO/NO_2 from <0.1 to 0.7 ± 0.3 ,
217 as well as and SO_2 from $<2 \text{ ppb}$ to $6.2 \pm 2.4 \text{ ppb}$. The large changes were expected

Formatted: Font: Symbol

Formatted: Font: Symbol

Formatted: Font: Symbol

Formatted: Font: Symbol

Formatted: Font: Symbol

Formatted: Font: Symbol

218 because the ship smoke stock was ~~only~~ approximately ~~only~~ 10 meters away from these
219 detectors. Thus, based upon the ~~feature~~~~features~~ described above, certain criteria were
220 designed in this study to identify ~~ship~~ self-~~ship~~-emission signals ~~so as~~ to separate ~~them~~
221 from ambient signals, i.e., a net increase in N_{cn} beyond $5 \times 10^4 \text{ cm}^{-3}$ in five minutes,
222 ~~the~~ median mobility mode diameter ~~around of approximately~~ 50 nm, $\text{NO}_2 > 30 \text{ ppb}$ and
223 $\text{NO}/\text{NO}_2 > 0.5$.

225 3. Results and discussion

226 3.1 Spatiotemporal variations in ambient N_{cn} during the cruise period—

227 Fig. 3 shows ~~at the~~ time series of minutely averaged distributions of N_{cn} , N_{cen} and AR at
228 ~~SSSSs~~ of 0.4% and 1.0% from DOY 110 to DOY 135 2018, ~~when—~~ after the ship self-
229 ~~ship~~-emission signals ~~had been exhaustedly~~ ~~were exhaustively~~ removed.—

231 When ~~the~~ spatiotemporal variations in N_{cn} were examined during the first half ~~of the~~
232 cruise period (Fig. 3a), ~~the it was found that~~ N_{cn} spanned a broad range of $0.2\text{--}4.5 \times 10^4$
233 cm^{-3} with ~~the an~~ average value of $8.1 \pm 4.4 \times 10^3 \text{ cm}^{-3}$. Specifically, ~~the~~ N_{cn} ~~were was~~
234 only $6.5 \pm 0.8 \times 10^3 \text{ cm}^{-3}$ at 00:00-06:00 LT on ~~DOY110~~ ~~DOY 110~~ when the ship
235 anchored at the Yangtze River estuary near Shanghai (Fig. 1). The low N_{cn} ~~values~~ were
236 comparable to the mean value of N_{cn} ($5.4 \times 10^3 \text{ cm}^{-3}$) in ~~the~~ marine-air cases during
237 January-December 2010 in Shanghai reported by Leng et al. (2013). The N_{cn}
238 ~~largely greatly~~ increased to $1.9 \pm 0.7 \times 10^4 \text{ cm}^{-3}$ at 08:00-21:00 LT on ~~DOY110~~ ~~DOY~~
239 ~~110~~ when the ship cruised across the Yangtze River estuary. The measured particles in
240 ~~the~~ number concentration were dominantly distributed ~~at in the~~ Aitken mode on that day,
241 while the median Aitken mode diameter shifted from $49 \pm 5 \text{ nm}$ at 00:00-06:00 to 40 ± 5
242 nm at 08:00-21:00 (Fig. S2). The Yangtze River estuary contains several world-class
243 ports and is heavily ~~travelled~~ ~~traveled~~ by marine ~~traffies~~ ~~traffic~~ in the daytime (Chen et
244 al., 2017). Since the onshore wind dominated on that day (not shown), the increase in
245 N_{cn} and the decrease in ~~the~~ median Aitken mode diameter at 08:00-21:00 LT possibly
246 reflected the increased contribution from marine traffic emissions. ~~Marine traffies~~ ~~The~~
247 ~~marine traffic~~ visibly decreased when the ship left the Yangtze River estuary toward the
248 south. The N_{cn} ~~were value~~ then significantly decreased, i.e., ~~to~~ $9.5 \pm 4.4 \times 10^3 \text{ cm}^{-3}$ in

Formatted: English (United States)

Formatted: English (United States)

Formatted: English (United States)

Formatted: English (United States)

Formatted: English (United States)

Formatted: English (United States)

Formatted: English (United States)

Formatted: English (United States)

Formatted: English (United States)

Formatted: English (United States)

Formatted: English (United States)

Formatted: English (United States)

Formatted: English (United States)

Formatted: English (United States)

Formatted: English (United States)

Formatted: English (United States)

Formatted: English (United States)

Formatted: English (United States)

Formatted: English (United States)

Formatted: English (United States)

Formatted: English (United States)

Formatted: English (United States)

Formatted: English (United States)

249 the marine atmosphere over the sea zone in Zhejiang Province (~~at~~for 07:00 LT on
250 ~~DOY111~~DOY 111 - 17:00 LT on DOY 114), with $P < 0.01$. The N_{cn} further decreased to
251 ~~the lower values of~~ $5.8 \pm 1.7 \times 10^3 \text{ cm}^{-3}$ in the marine atmosphere over the sea zone in
252 Fujian Province (~~at~~for 18:00 LT on ~~DOY114~~DOY 114 - 14:00 LT on DOY 117). All
253 these values were, however, 1-2 orders of magnitude ~~larger~~greater than the background
254 values in remote clear marine atmospheres, e.g., $< 300 \text{ particle cm}^{-3}$ without the
255 influence of industrial activities in the western Pacific and the tropical Pacific (Ueda et
256 al., 2016) and those reported by Quinn and Bates (2011) and Saliba et al. (2019),
257 indicating overwhelming contributions from ~~non-sea~~nonsea-spray aerosols including
258 marine traffic emissions, ~~the~~ long-range continental transport, newly formed particles
259 in marine atmospheres, etc. As reported, ~~atmospheric~~the atmospheric particles over
260 ~~China~~marginal seas in China can be further transported to the remote northwest Pacific
261 Ocean (NWPO) in spring under westerly winds, e.g., ~~the~~ N_{cn} observed over the NWPO
262 in March-April 2014 ~~were~~was as high as $2.8 \pm 1.0 \times 10^3 \text{ cm}^{-3}$ and
263 ~~approximately~~approximately half of that over ~~China~~marginal seas in China observed in
264 March 2014 (Wang et al., 2019).-

Formatted: English (United States)

Formatted: English (United States)

Formatted: English (United States)

Formatted: Font: Symbol

265
266 The mean value of N_{cn} ($8.1 \pm 4.4 \times 10^3$) observed in this study was close to that of 7.6
267 $\pm 4.0 \times 10^3 \text{ cm}^{-3}$ (the number concentrations of particles larger than 10 nm) observed
268 over the eastern part of the Yellow ~~sea~~Sea in spring 2017 ~~reported~~according by Park et
269 al. (2018). They attributed the high number concentrations of particles within
270 nucleation and Aitken modes to the long-range transport of air pollutants over eastern
271 China under the influence of westerly winds. Consistently, larger values of N_{cn} were
272 frequently observed in the continental atmospheres upwind of the Yellow ~~sea~~Sea, e.g.,
273 ~~the~~ mean values of $1.8 \pm 1.4 \times 10^4 \text{ cm}^{-3}$ in May 2013 in Qingdao, a coastal city in
274 proximity to the Yellow Sea (Li et al., 2015), $3.18 \times 10^4 \text{ cm}^{-3}$ in February-August 2014
275 in Beijing (Dal Maso et al., 2016), and $1.0 \times 10^4 \text{ cm}^{-3}$ in continental-air cases during
276 January-December 2010 in Shanghai (Leng et al., 2013).-

277

278 3.2 Spatiotemporal variations in ambient N_{cen} during the cruise period

279 N_{cen} data were generally available during the entire campaign (Fig. 3b). The mean
280 values of N_{cen} over ~~China~~marginal seas in China during ~~the~~DOY 110 to DOY 135,

281 2018 ~~were, ranged~~ from $3.2 \pm 1.1 \times 10^3 \text{ cm}^{-3}$ to $3.9 \pm 1.4 \times 10^3 \text{ cm}^{-3}$ under ~~SSSSs~~
282 ranging from 0.2% to 1.0% (Table 1), ~~which is~~ two to four times larger than the N_{cen}
283 at the same SS over the NWPO in March-April 2014 (Wang et al., 2019); and much
284 higher, i.e., 1-2 orders of magnitude, than the pristine marine background values (Quinn
285 and Bates, 2011). ~~As was~~ discussed in the previous section, the mean N_{cen} in this study
286 ($8.1 \pm 4.4 \times 10^3 \text{ cm}^{-3}$) was comparable to that of N_{cn} ($7.6 \pm 4.0 \times 10^3 \text{ cm}^{-3}$) over the
287 Yellow Sea in spring 2017 in Park et al. (2018); however, the comparison of ~~the~~ mean
288 N_{cen} reveals that ~~the~~ mean value ($3.6 \pm 1.2 \times 10^3 \text{ cm}^{-3}$) at SS of 0.6% in this study was
289 approximately 25% smaller than that ($4.8 \times 10^3 \text{ cm}^{-3}$ at ~~a~~ similar SS of 0.65%) in Park
290 et al. (2018), ~~which was~~ likely a result of long range transport, considering the
291 ~~observations made a~~ relatively ~~distant~~ long distance (i.e., 500-600 km) ~~observations~~
292 ~~away~~ from the land depicted in Fig. 1 of Park et al., 2018; and the subsequently higher
293 extent of aerosol aging. ~~The~~ N_{cen} under SS of 0.2% in this study ($3.2 \pm 1.1 \times 10^3$) is
294 comparable to that ($3.1 \pm 1.9 \times 10^3$) ~~by of~~ Li et al. (2015) in the continental atmosphere
295 of Qingdao in May 2013; however, the increment of N_{cen} with ~~the increase of~~ increasing
296 SS was much weaker in our study, resulting in ~~an~~ average of 36% smaller ~~in~~ N_{cen}
297 under ~~SSSSs~~ of 0.4% to 1.0% compared to ~~that of~~ Li et al. (2015). ~~Consistently, the~~ ~~The~~
298 sensitivity differences ~~of in~~ N_{cen} to SS between ~~the~~ relatively clean (i.e., N_{cn} (8.1 ± 4.4
299 $\times 10^3$) in this study) and polluted (with N_{cn} of $1.8 \pm 1.4 \times 10^4 \text{ cm}^{-3}$)
300 ~~environment~~ environments in Li et al. (2015) ~~is were~~ also reported by Nair et al. (2019),
301 who found little sensitivity ~~of in~~ N_{cen} to changes in SS over the equatorial Indian Ocean
302 ($< 6^\circ \text{N}$) with relatively clean air; and much larger enhancement of N_{cen} with ~~the increase~~
303 ~~of increasing~~ SS in polluted marine atmospheres ($> 6^\circ \text{N}$).

304
305 In addition, ~~the~~ N_{cen} at ~~SSSSs~~ from 0.1% to 1.0% during the period with high NH_4^+
306 (17:00 LT on DOY 114 to 10:00 LT on DOY 120) is statistically ~~significants~~ significantly
307 higher ($P < 0.01$) ~~in comparison to~~ than that during the poor NH_4^+ period (11:00 LT on
308 DOY 120 to 7:00 LT on DOY 136; Fig. 3b). More specifically, a large increase in
309 NH_4^+ concentration, with ~~a~~ mean concentration of $6.3 \pm 2.5 \mu\text{g m}^{-3}$, can be observed
310 during the period from 17:00 LT on DOY 114 to 10:00 LT on DOY 120 (Fig. 3b). The

311 mean N_{cen} during this period varied from $3.5 \pm 1.0 \times 10^3 \text{ cm}^{-3}$ to $4.0 \pm 1.1 \times 10^3 \text{ cm}^{-3}$ at
312 ~~SSSSs~~ ranging ~~effrom~~ 0.2% to 1.0%. In contrast, after DOY 120, the concentration of
313 NH_4^+ ($0.67 \pm 0.70 \mu\text{g m}^{-3}$) substantially decreased by almost 90%, during which the
314 mean N_{cen} at each SS showed statistically significant ~~decreased~~ decreases of 8% to 15%,
315 implicative of the vital contribution ~~to CCN~~ of secondary ammonium salt aerosols— to
316 CCN.

317

318 Another feature depicted in Fig. 3b is that the N_{cen} during the low NH_4^+ period may
319 even exceed the maximal value of N_{cen} during the high NH_4^+ period. To elucidate the
320 underlying mechanism, the N_{cen} values under each SS, ~~was~~ were composited and
321 compared ~~between~~ for the days with NH_4^+ ~~concentration~~ concentrations higher than the
322 upper quartile and the days in the lower quartile, yielding some interesting findings. At
323 SS=0.2%, the composited N_{cen} under the high NH_4^+ period was higher than that during
324 the low NH_4^+ period with a statistical significance level of 0.01. There was no
325 significant difference ~~in N_{cen}~~ between the N_{cen} values of the two ~~composited~~ composite
326 periods at SS values of 0.4% and 0.6%. However, the composited N_{cen} (i.e., only
327 selection of the upper quartile) during the high NH_4^+ period was significantly lower
328 than the composited value during the low NH_4^+ period ~~with~~ for $P < 0.01$, e.g., $5.1 \pm$
329 $0.5 \times 10^3 \text{ cm}^{-3}$ versus $5.3 \pm 0.7 \times 10^3 \text{ cm}^{-3}$ at SS=0.8%, % and $5.2 \pm 0.5 \times 10^3 \text{ cm}^{-3}$ versus
330 $5.7 \pm 0.7 \times 10^3 \text{ cm}^{-3}$ at SS =1.0%. During the low NH_4^+ period, the marine atmospheres
331 over the observational zones may sometimes receive strong continental inputs and/or
332 marine traffic emissions, leading to the larger N_{cen} . ~~Enhanced~~ The enhanced formation
333 of ammonium salt aerosols during the high NH_4^+ period likely canceled out or even
334 overwhelmed the effects of the continental inputs and/or marine traffic emissions ~~in~~
335 increasing N_{cen} at SS=0.2%.—

336 In addition, fresh marine traffic emissions likely ~~yielded~~ made a negligible contribution
337 to N_{cen} in the marine atmosphere because of ~~the~~ large ~~amount~~ amounts of aged aerosols
338 from various sources therein. For example, the mean values of N_{cen} were $3.2 \times 10^3 \text{ cm}^{-3}$
339 and $4.5 \times 10^3 \text{ cm}^{-3}$ at SS=0.4% and 1.0% at 08:30-11:30 on ~~DOY10~~ DOY 110,
340 respectively. ~~They~~ These values were almost the same as the $3.2 \times 10^3 \text{ cm}^{-3}$ at SS=0.4%

341 and $3.8 \times 10^3 \text{ cm}^{-3}$ at SS=1.0% before 06:00 on that day. The mean values of N_{cn} ,
342 however, ~~largely~~greatly increased from $6.5 \pm 0.8 \times 10^3 \text{ cm}^{-3}$ before 06:00 to $1.3 \pm$
343 $0.3 \times 10^4 \text{ cm}^{-3}$ at 08:30-11:30 when the ship cruised across the Yangtze River estuary
344 (Fig. 3b).—

Formatted: English (United States)

345

346 3.3 Spatiotemporal variations in CCN activation and Kappa values

347 The AR values at SSSs of 0.4% and 1.0% ~~were~~are examined in ~~the~~this section, as
348 shown in Fig. 3c. At SS=0.4%, the AR values largely varied from 0.06 to 0.92 with ~~the~~a
349 median value of 0.51. Specifically, the AR values narrowly varied around 0.51 ± 0.04
350 at 00:00-06:00 LT on ~~DOY110~~DOY 110. At 08:00-21:00 LT on that day, when the ship
351 cruised across the Yangtze River estuary, the AR values ~~were~~substantially decreased to
352 0.26 ± 0.06 concurrently with an approximate 200% increase in the N_{cn} values, i.e., N_{cn}
353 ~~value~~values of $6.5 \pm 0.8 \times 10^3 \text{ cm}^{-3}$ at 00:00-06:00 LT and $2.0 \pm 0.7 \times 10^4 \text{ cm}^{-3}$ at 08:00-
354 21:00 LT on ~~DOY110~~DOY 110 (Fig. 3a). The AR values then exhibited an oscillating
355 increase from DOY 111 to ~~DOY113~~DOY 113. A low AR ~~value~~value of $0.12 \pm$
356 0.04 ~~were~~was suddenly observed at 10:00-18:00 LT on ~~DOY114~~DOY 114 in the
357 presence of strong new particle signals transported from the upwind continental
358 atmosphere, as discussed later. The AR values, however, reached 0.34 ± 0.04 at 06:00-
359 08:00 LT and 0.39 ± 0.08 at 19:00-24:00 LT on ~~DOY114~~DOY 114, with the new particle
360 signals largely ~~reduced~~decreased. Even excluding the AR values on DOY 114, a
361 significant difference was still obtained between the AR values of 0.61 ± 0.12 during
362 the high NH_4^+ period and those of 0.55 ± 0.17 during the low NH_4^+ period.
363 ~~Enhanced~~The enhanced formation of ammonium salts seemingly increased the CCN
364 activity to some extent. At SS=1.0%, the AR values showed large
365 ~~fluctuation~~fluctuations with ~~the~~a median value of 0.57 ± 0.17 (Fig. 3c), and the
366 temporal trend was similar to that at SS=0.4%.—

Formatted: English (United States)

Formatted: English (United States)

Formatted: English (United States)

Formatted: English (United States)

Formatted: English (United States)

Formatted: English (United States)

Formatted: English (United States)

Formatted: English (United States)

367

368 To minimize the impact from the particle sizes, the Kappa values were further
369 investigated. As ~~was~~ reported by Phillips et al. (2018), Kappa values ~~in~~at a high time

370 resolution usually ~~exhibited~~exhibit a broad distribution, reflecting the complexity due
371 to various ~~of~~ factors. To reveal the key factors in determining the Kappa values ~~in~~on a
372 large spatiotemporal scale, the daily *Kappa* values of atmospheric aerosols were
373 estimated, on the basis of the daily mean N_{cen} and the size distributions of the particle
374 number concentration from ~~DOYDOYs~~ 110-118 (Fig. 3c). Please note that for DOY
375 110, considering the large differences ~~of~~in the particle number concentration between
376 00:00-06:00 and 08:00-21:00 (Fig. S2), the Kappa values ~~were~~ were calculated separately
377 for these two periods. At $SS=0.4\%$ (green dashed line in Fig. 3c), the estimated *Kappa*
378 values were as high as 0.66 at 00:00-06:00 LT, while ~~it~~they decreased to 0.37 at 08:00-
379 21:00 LT on ~~DOY110~~DOY 110. The *Kappa* value varied narrowly from 0.46 to 0.55
380 on ~~DOYDOYs~~ 111-113, 115 and 117, implying that inorganic aerosols such as
381 completely and incompletely neutralized ammonium salts may ~~yield~~make large
382 ~~contribution~~contributions to the N_{cen} . These values were generally consistent with the
383 reported observations in most ~~of~~ marine atmospheres. For example, Cai et al. (2017)
384 reported ~~the~~a *Kappa* value ~~around~~of approximately 0.5 for particles with sizes of 40-
385 200 nm at a marine site in Okinawa and ~~that~~ sulfate ~~to be~~was the dominant component
386 of aerosol particles on 1-9 November 2015, and a similar *Kappa* value in spring 2008
387 ~~over this site~~ was reported by Mochida et al. (2010) ~~over this site~~. Royalty et al. (2017)
388 reported *Kappa* values for 48, 96, and 144 nm dry particles ~~to be~~of 0.57 ± 0.12 , $0.51 \pm$
389 0.09 , and 0.52 ± 0.08 in the subtropical North Pacific Ocean and sulfate-like particles
390 contributing at most 77–88% to the total aerosol number concentration. ~~Kappa values~~
391 ~~over~~Over the Atlantic Ocean, ~~Kappa values of approximately~~ 0.54 ± 0.03 were
392 observed ~~around~~ 0.54 ± 0.03 for 284 nm particles (Phillips et al., 2018).-

393

394 The estimated *Kappa* values sometimes reached 0.66-0.67 (i.e., on DOY 116), which
395 may be related to unidentified factors. For example, O'Dowd et al. (2014) proposed that
396 some organics derived from sea-spray aerosols may also increase the N_{cen} , to some
397 extent, by reducing the surface ~~intension~~tension, leading to an increase ~~of~~in the *Kappa*
398 values. A small fraction of sea-salt aerosols in submicron particles may also increase
399 the *Kappa* values since its *Kappa* value was as high as 1.3 (O'Dowd et al., 1997;

Formatted: English (United States)

Formatted: English (United States)

Formatted: English (United States)

Formatted: English (United States)

Formatted: English (United States)

O'Dowd et al., 2004). ~~The~~ Kappa value of 0.29 was obtained on ~~DOY118,DOY 118,~~
which is close to the Kappa values widely observed for continental atmospheric
aerosols (~0.3) (Andreae and Rosenfeld, 2008; Poschl et al., 2009; Rose et al., 2010).
The estimated Kappa value largely decreased to 0.15 on ~~DOY114~~DOY 114 when new
particle formation (NPF) occurred, ~~with; see section 3.5 for~~ detailed discussion ~~in~~
~~section 3.5.~~ Moreover, at an SS of 1.0%, the estimated Kappa value was always smaller
than 0.2. The Kappa ~~value~~values of organics ~~was~~were commonly assumed ~~as to be~~ 0.1
(Rose et al., 2011; Cai et al., 2017; Singla et al., 2017). In general, the fraction of
organics in the nanometer particles increases with decreasing particle ~~size~~size, from
~~~100 nm to~~ 40-50 nm~50 nm (Rose et al., 2010; Rose et al., 2011; Crippa et al., 2014;  
Cai et al., 2017). A combination of the two factors likely led ~~to~~the overall Kappa values  
estimated at SS=1.0% to be much lower. However, ~~the~~ direct measurements of the  
chemical composition of nanometer particles are needed to confirm ~~the~~these arguments.

413

#### 3.4 Particle number size distributions and CCN activation associated with marine traffic emissions and aerosol aging

The particle number size distributions during ~~DOY~~DOYs 110-118, shown in Fig. 4, can  
be ~~in general~~generally classified into two categories. Category 1 occurred on  
~~DOY110~~DOYs 110-114, when particle number concentrations were mainly distributed  
~~at the~~in Aitken mode, whereas the accumulation mode was generally undetectable.  
Category 2 occurred on ~~DOY115~~DOYs 115-118, when the accumulation mode  
~~can~~could be clearly identified and generally dominated over the Aitken mode. Hoppel  
(1986) proposed that cloud-modified aerosols ~~to be~~are mainly distributed at 80-150 nm  
in the remote tropical Atlantic and Pacific oceans. Cloud-modified aerosols are quite  
common in remote marine ~~atmosphere~~atmospheres, likely leading to the  
~~dominated~~dominant accumulation mode particles ~~to be~~being observed on  
~~DOY115~~DOYs 115-118. Occasionally, the Aitken mode dominated over the  
accumulation mode ~~on some day~~, such as on DOY 118. To further ~~dive into~~investigate  
the sources of different modes of particles, three ~~day~~days of ~~DOY112~~DOY 112, DOY

Formatted: Not Highlight

Formatted: Not Highlight

Formatted: Font color: Text 1

Formatted: Font: Not Bold, Font color: Text 1, Not Highlight

Formatted: Font: Not Bold, Font color: Text 1, Not Highlight

Formatted: Font color: Text 1



429 116 and ~~DOY118~~DOY 118 were selected.—

430

431 On DOY 112, the Aitken mode particles accounted for approximately 60% of the total

432 particle number concentration (Fig. 5a), with median Aitken mode diameters ~~around of~~

433 ~~approximately~~  $54 \pm 8$  nm, ~~Like~~Similar to the observations over the Yangtze River estuary,

434 the mean value of  $N_{cn}$  increased by approximately 50% concurrently with a decrease in

435 the median Aitken mode diameters by  $\sim 9$  nm at 05:30 – 11:40 LT ~~against~~compared to

436 those ~~at~~in the early morning before 05:30 LT (Fig. 5b).— Concomitantly, the AR values

437 decreased to  $0.31 \pm 0.09$  at SS of 0.4%, with similar AR ~~decreased~~decreases at SS of 1.0%,

438 and the lowest AR and *Kappa* values ~~occurring~~occurred at 06:00-07:00 LT at ~~SSSSs~~ of

439 both 0.4% and 1.0%. All these results ~~pointed towards~~indicated that the increase in

440 Aitken mode particles at 05:30 – 11:40 LT ~~to be~~was likely derived from enhanced

441 marine traffic contributions carried by the onshore wind from the south (Fig. S11).

442 During other ~~time~~times on ~~DOY112~~DOY 112, the onshore wind may also carry ~~the~~

443 ~~marine-traffic-derived~~ particles to the observational sea zones. However, the marine-

444 ~~traffic-derived~~ particles likely aged to some extent, e.g., the median Aitken mode

445 diameters exhibited an oscillating increase from approximately 50 nm at 19:00 to

446 approximately 70 nm at 24:00 LT with ~~the~~a particle growth rate of  $\sim 4$  nm hour<sup>-1</sup>. The

447 AR values, however, narrowly varied around  $0.47 \pm 0.03$  at SS=0.4% and  $0.52 \pm 0.05$  at

448 SS=1.0% during the particle growth period. The *Kappa* values at SS=0.4% gradually

449 decreased from 0.56 at 19:00 to 0.41 at 23:00 LT, reflecting more aged marine-

450 ~~traffic-~~derived particles growing into CCN ~~size-sizes~~.

451

452 On DOY 116, the accumulation mode particles ~~instead of Aitken mode particles~~

453 dominantly contributed to  $N_{cn}$  ~~rather than Aitken mode particles~~ (Fig. 5d),— under the

454 marine air influence from the northeast (Fig. S13). The median accumulation mode

455 diameters narrowly varied around  $135 \pm 5$  nm at 01:00-13:00 LT and  $102 \pm 5$  nm at 16:20-

456 24:00 LT with ~~the~~a transition period in between (Fig. 5e). The AR and *Kappa* values,

457 however, showed no statistically significant ~~differene~~differences during the two

458 periods at ~~SSSSs~~ of 0.4% and 1.0%, implying that the size change in ~~the~~ accumulation

Formatted: Font: Symbol

Formatted: Font color: Black

Formatted: English (United States)

Formatted: Font color: Black

Formatted: Font: Symbol

Formatted: Font color: Black

Formatted: Font color: Black

Formatted: Font color: Black

Formatted: Font: Symbol

Formatted: Font: Symbol

Formatted: Font color: Black

Formatted: Font: Symbol

Formatted: Font: Symbol

459 mode particles ~~showed~~had a negligible influence on ~~the~~CCN activation. ~~Hourly~~The  
460 ~~hourly~~ variations in ~~the~~AR and *Kappa* values may be associated with other factors, e.g.,  
461 chemical composition, ~~and~~ mixing state, ~~etc.~~ (Gunthe et al., 2011; Rose et al., 2011).–

462

463 On DOY 118, under the influence of ~~mixture~~mixtures from ~~the~~ marine and coastal areas  
464 from the northeast (Fig. S14), the accumulation mode particles generally dominated the  
465 contribution to  $N_{cn}$ , while the reverse was true ~~in~~on some occasions (Fig. 5g,h). The  
466 median accumulation mode diameters exhibited an oscillating increase from  
467 approximately 100 nm to 130 nm at 00:00-08:00 LT, narrowly varied around  $133 \pm 5$  nm  
468 at 08:00-13:00 LT, and then exhibited an oscillating decrease down to approximately  
469 100 nm at 20:00 LT. The AR values and *Kappa* values at SS=0.4%, however, exhibited  
470 an inverted bell-shape with the lowest values at 0.31 and 0.11 at 13:00. The decreases  
471 in ~~the~~AR values and *Kappa* may be related to organic ~~econdensed~~condensation on ~~the~~  
472 accumulation mode particles since the median accumulation mode diameters were  
473 almost ~~the~~ largest at 13:00. The number concentration of Aitken mode particles ~~was~~  
474 evidently enhanced at 14:00-15:00, but the influence on ~~the~~AR values and *Kappa*  
475 values at SS=0.4% was undetectable (Fig. 5i).–

476

### 477 3.5 The long-range transport of ~~new grown~~ new particles on DOY 114

478 No hour-long sharp ~~increase~~increases were observed in ~~the~~ number concentration of  
479 ~~the~~ nucleation mode particles (< 20 nm) ~~was observed~~during the period from DOY 110  
480 to DOY 118, except on ~~DOY 114~~DOY 114 (Fig. 4). According to the conventional  
481 definition of NPF events (Kulmala et al., 2004; Dal Maso et al., 2005), the occurrence  
482 frequency of NPF events was low in this study. Unlike continental atmospheres where  
483 a high occurrence frequency of NPF events has been observed globally in spring  
484 (Kulmala et al., 2004; Kerminen et al., 2018), a low occurrence frequency reportedly  
485 occurred over the seas during the “Meiyu (plum-rain) season” in spring because of  
486 frequent rainy, foggy or cloudy weather conditions (Zhu et al., 2019). ~~Lack~~The lack of  
487 NPF events in the marine atmospheres implied ~~that the contributions to~~  $N_{cn}$  and  $N_{cen}$  ~~to~~

488 ~~be were~~ mainly ~~contributed by primarily from primary~~ emitted aerosols and their aged  
489 products.—

490 During the period of 10:00-18:00 LT on DOY 114, ~~a~~the large increase in ~~the~~ number  
491 concentrations of Aitken mode particles (Fig. 6a) likely reflected the long-range  
492 transport of ~~new~~ grown ~~new~~-particles from upwind continental atmospheres (Fig. S12).  
493 The size distributions of ~~the~~ particle number concentration showed a dominant Aitken  
494 mode at 10:00-18:00 LT, when ~~the~~ spatiotemporal variations in  $N_{cn}$  and median Aitken  
495 mode diameters exhibited bell-~~shapeshaped~~ patterns (Fig. 6b). The median Aitken  
496 mode diameters increased from 26 nm at 10:00 LT to 33 nm at 12:00-13:00 LT and then  
497 decreased to 20 nm prior to the signal disappearance, likely reflecting the growth and  
498 shrinkage of the Aitken mode particles (Yao et al., 2010; Zhu et al., 2019). The median  
499 Aitken mode diameters were evidently smaller than the values, i.e., 40-50 nm for ~~the~~  
500 Aitken mode particles, observed over ~~the~~ Yangtze River estuary on DOY 112 (Fig. 5a).

501 Moreover, the number concentrations of ~~the~~ 20-40 nm particles increased by 5.8 times  
502 at 12:00-13:00 LT compared to the mean value at 06:00-09:00 LT, while the total  
503 number concentrations of particles greater than 90 nm increased by only 67%. These  
504 results implied ~~that the largely increased~~large increases in ~~the~~ number concentrations  
505 of Aitken mode ~~particles~~ with a dynamic change in ~~the~~ mode diameter observed at  
506 10:00-18:00 LT ~~unlikely to be were not likely~~ caused by ~~primarily primary~~ emitted and  
507 aged particles from marine traffic emissions or other combustion sources. The  
508 observations of ~~the~~ gaseous and particulate species, during the same period, implied  
509 ~~that the~~ air masses ~~to be were~~ well-aged and less polluted. For instance, the measured  
510 hourly average mixing ratios of  $SO_2$  ~~was were~~ no larger than 1.2 ppb (Fig. 6c), and the  
511 hourly average concentrations of  $NH_4^+$  in  $PM_{2.5}$  were smaller than  $2 \mu g m^{-3}$  (Fig. 3b).  
512 In addition, the concentrations of  $K^+$  were below  $0.3 \mu g m^{-3}$ , suggesting negligible  
513 contributions from biomass burning (Fig. 6e).—

514  
515 Before 09:00 LT, a much weaker spike of nucleation mode particles was intermittently  
516 observed (Fig. 6a). The weak and intermittent NPF ~~seems seemed~~ to occur in the marine  
517 atmospheres before 09:00 LT when no apparent growth of new particles was observed.

Formatted: Font color: Black

Formatted: English (United States)

Formatted: English (United States)

Formatted: English (United States)

Formatted: English (United States)

Formatted: English (United States)

Formatted: English (United States)

Formatted: English (United States)

Formatted: English (United States)

Formatted: English (United States)

Formatted: English (United States)

Formatted: English (United States)

518 Possibly due to ~~the~~ transport from the continent (Fig. S12) and an increase in the  
519 condensational sink ~~around~~ at approximately 10:00 am (Fig. 6a), the weak NPF signal  
520 gradually dropped to a negligible level half an hour later, concomitant with a large  
521 increase in the number concentrations of Aitken mode ~~particles~~ at 10:00-18:00 LT.—

Formatted: English (United States)

Formatted: English (United States)

522  
523  $N_{cen}$  at SS=0.4% increased from  $1.2 \times 10^3 \text{ cm}^{-3}$  at 06:00-09:00 LT to the peak value of  
524  $2.3 \times 10^3 \text{ cm}^{-3}$  at 12:00 LT, with an increase of 92%, and  $N_{cen}$  at SS=1.0% increased  
525 from  $1.6 \times 10^3 \text{ cm}^{-3}$  to  $4.0 \times 10^3 \text{ cm}^{-3}$ , with an increase of 150% (Fig. 6d). The net  
526 increase in  $N_{cen}$  at SS=0.4% likely reflected the contribution from pre-existing particles  
527 since new particles with ~~the diameter~~ diameters less than 50 nm were unlikely to be  
528 activated as CCN at such low SS (Li et al., 2015; Wu et al., 2016; Ma et al., 2016). The  
529 larger net increase in  $N_{cen}$  at SS=1.0% may reflect the contributions ~~mixed~~ from pre-  
530 existing particles and new grown ~~new~~ particles. The high SS can activate particles as  
531 CCN with diameters down to 40 nm (Dusek et al., 2006; Li et al., 2015). The invasion  
532 of new grown ~~new~~ particles also led to the large decreases in the AR values largely  
533 ~~decreased~~ from 0.3 to 0.1 at SS=0.4%, ~~%~~ and from 0.4 to 0.2 at SS=1.0% (Fig. 6e). After  
534 18:00 LT, the AR values returned to 0.3-0.4 at SS=0.4% and 0.4-0.6 at SS=1.0%. ~~When~~  
535 ~~the~~ The calculated *Kappa* values were examined (Fig. ~~6e~~), ~~they decreased~~ 6c and ~~were~~  
536 found to decrease from 0.4 to 0.1-0.2 at SS=0.4%. ~~The~~ This value returned to 0.3 at  
537 18:00-19:00 LT (FMPS ~~was~~ temporarily malfunctioned after 19:20 LT). The *Kappa*  
538 values were below 0.2 at SS=1.0% on that day. The decreases in the AR values and  
539 *Kappa* values at the two SS were likely caused by organic vapor condensed on  
540 preexisting particles and new particles (Wu et al., 2016; Zhu et al., 2019).—

541

542 3.6 Correlations ~~Relationship~~ Relationship of  $N_{cn}$  and  $N_{ccn}$  with  $SO_2$  in ship self-ship  
543 plumes and ambient air—

544 When ship self-ship emission signals were detected, the observational values included  
545 a combination of contributions from ship self-ship emissions and ambient  
546 concentrations. Although the ambient  $N_{cn}$  was negligible in comparison with the  $N_{cn}$

547 derived from ~~the ship self-ship~~ emissions, ~~it~~this was not the case for  $N_{cen}$  and  $SO_2$ .  
548 Based on the ~~minutely per minute~~ data, the signal was considered ~~as to be~~ vessel-self  
549 ~~emission-emissions~~ when both  $N_{cn}$  ~~was~~ greater than  $50,000 \text{ cm}^{-3}$  and  $SO_2$  ~~was~~ greater  
550 than 5 ppb. The composited data ~~was/were~~ then used to derive the hourly average  $N_{cn}$ ,  
551  $N_{cen}$  and  $SO_2$ , which was then subtracted by the ambient hourly mean value during the  
552 preceding hour with relatively clean conditions (i.e., ~~eonecentration~~~~concentrations~~ of  $N_{cn}$   
553 lower than  $10,000 \text{ cm}^{-3}$ ; ~~and~~  $SO_2$  lower than 2.5 ppb). Please note ~~that~~ uncertainties  
554 exist in terms of the criteria and separation between ~~the ship self-shipsignals~~ and  
555 ambient signals; however, minimal impact is expected in the relationship examined  
556 below.

557

558 Fig. 7a ~~showed correlations~~shows the relationship of  $N_{cn}$  and  $N_{cen}$  with ~~the~~ mixing ratio  
559 of  $SO_2$  in ~~the ship self-ship~~ plumes, prefixed by  $\Delta$  for  $N_{cn}$ ,  $N_{cen}$  and  $SO_2$  to implicate the  
560 removal of ambient signals. A good correlation of 0.66 for  $R^2$  ( $P < 0.01$ ) ~~was~~is obtained,  
561 and the slope indicates that  ~~$N_{cen}$~~ the increase ~~in~~  $N_{cn}$  by  $1.4 \times 10^4 \text{ cm}^{-3}$  for each ppb  
562 increase ~~of~~in  $SO_2$  resulted from ship ~~emission~~emissions (Fig. 7a). High emissions of  
563  $N_{cn}$  were generally reported in engine exhausts ~~with~~where high sulfur-content diesel ~~to~~  
564 ~~be~~was used (Yao et al., 2005; Yao et al., 2007). ~~In regard of~~The  $N_{cen}$  at SS of 0.2% to  
565 1.0% (Fig. 7b), ~~it increases~~ increased from  $30 \text{ cm}^{-3}$  to  $170 \text{ cm}^{-3}$  per 1 ppb increase ~~of~~in  
566  $SO_2$ , showing ~~statistica~~a statistically significant correlation at ~~the~~ 99<sup>th</sup> confidence level.  
567 The contribution ~~ratio~~ratios of  $SO_2$  to  $N_{cen}$  ~~is~~were 0.002 (SS of 0.2%), 0.004 (SS of  
568 0.4%) and 0.012 (SS of 1.0%) to that of  $N_{cn}$ , ~~which is~~ in general consistent with ~~the~~a  
569 previous study by Ramana and Devi (2016), in which a range of 0.0012–0.57 was  
570 observed for CCN at 0.4% in Bay of Bengal during Aug 13–16, 2012.–

571

572 The ~~correlations~~relationship of hourly averaged  $N_{cn}$  and  $N_{cen}$  with  $SO_2$  in ambient air  
573 were examined and ~~showed~~are shown in Fig. 7c, d. The data ~~was/were~~ segmented into  
574 pieces based on  $SO_2$  with ~~an~~ interval of 0.2 ppb. A good correlation ~~was obtained~~  
575 between the averaged  $N_{cn}$  and  $SO_2$  ~~were obtained~~– with ~~an~~  $R^2$  of 0.80 ( $P < 0.01$ ), and ~~a~~

576 1 ppb increase in SO<sub>2</sub> likely increased N<sub>cen</sub> by 1.6 × 10<sup>3</sup> cm<sup>-3</sup> (Fig. 7c). The increase in  
577 N<sub>cen</sub> with SO<sub>2</sub> may reflect the contribution from primary emissions. ~~As~~The intercept was,  
578 however, as large as 3.9 × 10<sup>3</sup> cm<sup>-3</sup>, likely representing the contribution from well-aged  
579 aerosols. —

580  
581 ~~Hourly~~The hourly averaged N<sub>cen</sub> at different SS generally increased with ~~increase~~  
582 ~~of increasing~~ ambient SO<sub>2</sub> (Fig. 7d). A good correlation was obtained between the  
583 averaged N<sub>cen</sub> and SO<sub>2</sub> ~~were obtained,~~ with R<sup>2</sup>=0.78-0.91 (P<0.01). ~~A~~ 1 ppb increase  
584 in SO<sub>2</sub> likely increased N<sub>cen</sub> by 0.6 × 10<sup>3</sup> to 0.8 × 10<sup>3</sup> cm<sup>-3</sup> at ~~SSSSs~~ from 0.2% to 1.0%.  
585 The increase in N<sub>cen</sub> with SO<sub>2</sub> may also reflect the contribution from primary emissions.  
586 The intercepts of 2.2 × 10<sup>3</sup>-2.7 × 10<sup>3</sup> cm<sup>-3</sup> at different SS were likely contributed by  
587 well-aged aerosols. ~~The~~This relationship may be used as an estimation of ~~the~~ N<sub>cen</sub> in  
588 marine atmospheres over ~~China~~ marginal seas, in China when no measurements of CCN  
589 ~~were~~are available, whereas ~~the~~ ambient SO<sub>2</sub> can be estimated from web-based satellite  
590 data. —

#### 591 4. Conclusions

592 ~~Spatiotemporal~~The spatiotemporal variations in ambient N<sub>cn</sub> and N<sub>cen</sub> were studied  
593 during a cruise campaign on ~~DOYDOYS~~ 110-135 over ~~China~~ marginal seas in China.  
594 The mean values of N<sub>cn</sub> (8.1 × 10<sup>3</sup> cm<sup>-3</sup>) and N<sub>cen</sub> (3.2-3.9 × 10<sup>3</sup> cm<sup>-3</sup>) at ~~SSSSs~~ of 0.2%-  
595 1.0% were approximately one order of magnitude larger than those in remote clear  
596 marine atmospheres, indicating overwhelming contributions from ~~non-sea~~nonsea-spray  
597 aerosols such as marine traffic emissions, ~~the~~ long-range continental transport and  
598 others.

599  
600 ~~Observed~~The observed ship self-ship-emission signals showed ~~that~~ fresh marine traffic  
601 emissions can be important sources of N<sub>cn</sub>, but ~~a~~ minor ~~sources~~sources of N<sub>cen</sub> in the  
602 marine atmosphere. The signals showed that ~~a~~ 1 ppb increase in SO<sub>2</sub>  
603 ~~corresponds~~corresponded to ~~a~~ 1.4 × 10<sup>4</sup> cm<sup>-3</sup> increase in N<sub>cn</sub> and ~~a~~ 30-170 cm<sup>-3</sup> increase  
604 in N<sub>cen</sub> at SS=0.2-1.0%. Data analysis showed that marine traffic emissions largely

Formatted: Font color: Black

605 increased  $N_{\text{cen}}$  over ~~their~~ heavily ~~travelled~~traveled sea zones in the daytime.—

606

607 In ambient marine air, the growth of marine traffic–derived particles led to a decrease  
608 in the estimated bulk kappa values at 0.4%~~%,~~ possibly because some of these particles  
609 enriched in organics grew into CCN size. However, strong formation of ammonium  
610 salts led to aerosol aging, and significantly increased  $N_{\text{cen}}$  at SS of 0.2-1.0% in  
611 comparison with those observed during the period poor in ammonium salt aerosols in  
612  $\text{PM}_{2.5}$  with  $P < 0.01$ . The estimated bulk Kappa values from the daily average values  
613 varied from 0.46 to 0.55 at SS=0.4% in most ~~of~~ marine atmospheres, indicating that  
614 inorganic ammonium aerosols may dominantly contribute to the  $N_{\text{cen}}$  at SS of 0.4%.

615 The particle number size distributions showed that the high bulk Kappa values could  
616 be related to cloud-modified aerosols, which likely led to a large extent of degradation  
617 of organics and ~~subsequently lost~~subsequent loss from the particle phase.—

618

619 ~~Humid marine ambient air led to~~ NPF events rarely ~~occurring therein~~occurred in the  
620 humid ambient marine air. The dominant onshore winds occurred during most of the  
621 measurement periods, and ~~should carry~~likely carried primary aerosols and their aged  
622 products rather than secondarily formed aerosols to the observational zone. During an  
623 occasion when offshore winds blew from the northwest (Fig. S12), new particle signals  
624 transported from the continent can be clearly observed. However, the NPF in the marine  
625 atmosphere was too weak to be important. The new transported ~~new~~ particles from the  
626 continent yielded the maximal ~~increase~~increases in  $N_{\text{cen}}$  ~~by of~~ 92% at SS of 0.4% and  
627 150% at SS of 1.0%. However, consistent with those reported in the literature, the  
628 estimated ~~kappa~~Kappa values largely decreased from 0.4 to 0.1-0.2 at SS=0.4% during  
629 most ~~time~~—of the continent ~~transported~~transporting NPF event because ~~of~~—the  
630 ~~kappa~~Kappa value of the organic condensation vapor was as low as 0.1.—

631

632 **Competing interests.** The authors declare that they have no conflict of interest.

633 **Author contributions.** YG and XY designed the research, YG, DZ and XY performed

Formatted: English (United States)

Formatted: English (United States)

Formatted: English (United States)

Formatted: Font color: Black

---

634 the analysis, JW and HG helped on the interpretation of the results, and all co-authors  
635 contributed to the writing of the paper.

636 **Acknowledgment**

637 This research is supported by the National Key Research and Development Program in  
638 China (grant no. 2016YFC0200504) and the Natural Science Foundation of China  
639 (grant no. 41576118).

640

641 **References**

642 Andreae, M. O., and Rosenfeld, D.: Aerosol-cloud-precipitation interactions. Part 1. The  
643 nature and sources of cloud-active aerosols, *Earth-Sci. Rev.*, 89, 13-41,  
644 10.1016/j.earscirev.2008.03.001, 2008.

645 Blot, R., Clarke, A. D., Freitag, S., Kapustin, V., Howell, S. G., Jensen, J. B., Shank, L.  
646 M., McNaughton, C. S., and Brekhovskikh, V.: Ultrafine sea spray aerosol over the  
647 southeastern Pacific: open-ocean contributions to marine boundary layer CCN,  
648 *Atmos. Chem. Phys.*, 13, 7263-7278, 10.5194/acp-13-7263-2013, 2013.

649 Bougiatioti, A., Fountoukis, C., Kalivitis, N., Pandis, S. N., Nenes, A., and Mihalopoulos,  
650 N.: Cloud condensation nuclei measurements in the eastern Mediterranean marine  
651 boundary layer: CCN closure and droplet growth kinetics, *Atmos. Chem.*  
652 *Phys. Discuss.*, 9, 10303-10336, 10.5194/acpd-9-10303-2009, 2009.

653 Brooks, S. D., and Thornton, D. C. O.: Marine Aerosols and Clouds, *Annu. Rev. Mar.*  
654 *Sci.*, 10, 289-313, 10.1146/annurev-marine-121916-063148, 2018.

655 Cai, M. F., Tan, H. B., Chan, C. K., Mochida, M., Hatakeyama, S., Kondo, Y., Schurman,  
656 M. I., Xu, H. B., Li, F., Shimada, K., Li, L., Deng, Y. G., Yai, H., Matsuki, A., Qin,  
657 Y. M., and Zhao, J.: Comparison of Aerosol Hygroscopicity, Volatility, and Chemical  
658 Composition between a Suburban Site in the Pearl River Delta Region and a Marine  
659 Site in Okinawa, *Aerosol. Air. Qual. Res.*, 17, 3194-3208,  
660 10.4209/aaqr.2017.01.0020, 2017.

661 Charlson, R. J., Lovelock, J. E., Andreae, M. O., and Warren, S. G.: Oceanic  
662 phytoplankton atmospheric sulphur cloud albedo and climate, *Nature*, 326, 655-661,



---

663 1987.

664 Chen, D. S., Wang, X. T., Li, Y., Lang, J. L., Zhou, Y., Guo, X. R., and Zhao, Y. H.: High-  
665 spatiotemporal-resolution ship emission inventory of China based on AIS data in  
666 2014, *Sci. Total Environ.*, 609, 776-787, 10.1016/j.scitotenv.2017.07.051, 2017.

667 Cheung, H. C., Chou, C. C.-K., Lee, C. S. L., Kuo, W.-C., and Chang, S.-C.:  
668 Hygroscopic properties and cloud condensation nuclei activity of atmospheric  
669 aerosols under the influences of Asian continental outflow and new particle  
670 formation at a coastal site in eastern Asia, *Atmos. Chem. Phys.*, 20, 5911–5922,  
671 <https://doi.org/10.5194/acp-20-5911-2020>, 2020.

672 Clarke, A. D., Owens, S. R., and Zhou, J. C.: An ultrafine sea-salt flux from breaking  
673 waves: Implications for cloud condensation nuclei in the remote marine atmosphere,  
674 *J. Geophys. Res.-Atmos.*, 111, Artn D06202, 10.1029/2005jd006565, 2006.

675 Crippa, M., Canonaco, F., Lanz, V. A., Aijala, M., Allan, J. D., Carbone, S., Capes, G.,  
676 Ceburnis, D., Dall'Osto, M., Day, D. A., DeCarlo, P. F., Ehn, M., Eriksson, A., Freney,  
677 E., Hildebrandt Ruiz, L., Hillamo, R., Jimenez, J. L., Junninen, H., Kiendler-Scharr,  
678 A., Kortelainen, A. M., Kulmala, M., Laaksonen, A., Mensah, A., Mohr, C., Nemitz,  
679 E., O'Dowd, C., Ovadnevaite, J., Pandis, S. N., Petaja, T., Poulain, L., Saarikoski, S.,  
680 Sellegri, K., Swietlicki, E., Tiitta, P., Worsnop, D. R., Baltensperger, U., and Prevot,  
681 A. S. H.: Organic aerosol components derived from 25 AMS data sets across Europe  
682 using a consistent ME-2 based source apportionment approach, *Atmos. Chem. Phys.*,  
683 14, 6159-6176, 10.5194/acp-14-6159-2014, 2014.

684 Dal Maso, M., Kulmala, M., Riipinen, I., Wagner, R., Hussein, T., Aalto, P. P., and  
685 Lehtinen, K. E. J.: Formation and growth of fresh atmospheric aerosols: eight years  
686 of aerosol size distribution data from SMEAR II, Hyytiala, Finland, *Boreal Environ.*  
687 *Res.*, 10, 323-336, 2005.

688 Dal Maso, M., Gao, J., Jarvinen, A., Li, H., Luo, D. T., Janka, K., and Ronkko, T.:  
689 Improving Urban Air Quality Measurements by a Diffusion Charger Based Electrical  
690 Particle Sensors - A Field Study in Beijing, China, *Aerosol. Air. Qual. Res.*, 16, 3001-  
691 3011, 10.4209/aaqr.2015.09.0546, 2016.

692 Decesari, S., Finessi, E., Rinaldi, M., Paglione, M., Fuzzi, S., Stephanou, E. G., Tzias,

---

693 T., Spyros, A., Ceburnis, D., O'Dowd, C., Dall'Osto, M., Harrison, R. M., Allan, J.,  
694 Coe, H., and Facchini, M. C.: Primary and secondary marine organic aerosols over  
695 the North Atlantic Ocean during the MAP experiment, *J. Geophys. Res.-Atmos.*, 116,  
696 Artn D22210,10.1029/2011jd016204, 2011.

697 Ding, X., Qi, J. H., and Meng, X. B.: Characteristics and sources of organic carbon in  
698 coastal and marine atmospheric particulates over East China, *Atmos. Res.*, 228, 281-  
699 291, 10.1016/j.atmosres.2019.06.015, 2019.

700 Dusek, U., Frank, G. P., Hildebrandt, L., Curtius, J., Schneider, J., Walter, S., Chand, D.,  
701 Drewnick, F., Hings, S., Jung, D., Borrmann, S., and Andreae, M. O.: Size matters  
702 more than chemistry for cloud-nucleating ability of aerosol particles, *Science*, 312,  
703 1375-1378, 10.1126/science.1125261, 2006.

704 Feng, J. L., Guo, Z. G., Zhang, T. R., Yao, X. H., Chan, C. K., and Fang, M.: Source and  
705 formation of secondary particulate matter in PM<sub>2.5</sub> in Asian continental outflow, *J.*  
706 *Geophys. Res.-Atmos.*, 117, Artn D03302,10.1029/2011jd016400, 2012.

707 Feng, L., Shen, H., Zhu, Y., Gao, H., and Yao, X.: Insight into Generation and Evolution  
708 of Sea-Salt Aerosols from Field Measurements in Diversified Marine and Coastal  
709 Atmospheres, *Sci. Rep.*, 7, 41260, 10.1038/srep41260, 2017.

710 Feng, T., Li, G. H., Cao, J. J., Bei, N. F., Shen, Z. X., Zhou, W. J., Liu, S. X., Zhang, T.,  
711 Wang, Y. C., Huang, R. J., Tie, X. X., and Molina, L. T.: Simulations of organic  
712 aerosol concentrations during springtime in the Guanzhong Basin, China, *Atmos.*  
713 *Chem. Phys.*, 16, 10045-10061, 10.5194/acp-16-10045-2016, 2016.

714 Fossum, K. N., Ovadnevaite, J., Ceburnis, D., Dall'Osto, M., Marullo, S., Bellacicco, M.,  
715 Simo, R., Liu, D. T., Flynn, M., Zuend, A., and O'Dowd, C.: Summertime Primary  
716 and Secondary Contributions to Southern Ocean Cloud Condensation Nuclei, *Sci.*  
717 *Rep.*, 8, Artn 13844,10.1038/S41598-018-32047-4, 2018.

718 Fu, X. G., Wang, M., Zeng, S. Q., Feng, X. L., Wang, D., and Song, C. Y.: Continental  
719 weathering and palaeoclimatic changes through the onset of the Early Toarcian  
720 oceanic anoxic event in the Qiangtang Basin, eastern Tethys, *Palaeogeogr. Palaeocl.*,  
721 487, 241-250, 10.1016/j.palaeo.2017.09.005, 2017.

722 Gunthe, S. S., Rose, D., Su, H., Garland, R. M., Achtert, P., Nowak, A., Wiedensohler,

---

723 A., Kuwata, M., Takegawa, N., Kondo, Y., Hu, M., Shao, M., Zhu, T., Andreae, M.  
724 O., and Pöschl, U.: Cloud condensation nuclei (CCN) from fresh and aged air  
725 pollution in the megacity region of Beijing, *Atmos. Chem. Phys.*, 11, 11023-11039,  
726 10.5194/acp-11-11023-2011, 2011.

727 Guo, L., Chen, Y., Wang, F., Meng, X., Xu, Z., and Zhuang, G.: Effects of Asian dust on  
728 the atmospheric input of trace elements to the East China Sea, *Mar. Chem.*, 163, 19-  
729 27, 10.1016/j.marchem.2014.04.003, 2014.

730 Guo, T., Li, K., Zhu, Y., Gao, H., and Yao, X.: Concentration and size distribution of  
731 particulate oxalate in marine and coastal atmospheres – Implication for the increased  
732 importance of oxalate in nanometer atmospheric particles, *Atmos. Environ.*, 142, 19-  
733 31, 10.1016/j.atmosenv.2016.07.026, 2016.

734 Hoppel W. A., F. G. M., and Larson R. E.: Effect of non-precipitating clouds on the  
735 aerosol size distribution, *Geophys. Res. Lett.*, 13, 125-128, 1986.

736 Huebert, B. J., Bates, T., Russell, P. B., Shi, G. Y., Kim, Y. J., Kawamura, K., Carmichael,  
737 G., and Nakajima, T.: An overview of ACE-Asia: Strategies for quantifying the  
738 relationships between Asian aerosols and their climatic impacts, *J. Geophys. Res.-*  
739 *Atmos.*, 108, Artn 8633, 10.1029/2003jd003550, 2003.

740 Hung, H. M., Lu, W. J., Chen, W. N., Chang, C. C., Chou, C. C. K., and Lin, P. H.:  
741 Enhancement of the hygroscopicity parameter kappa of rural aerosols in northern  
742 Taiwan by anthropogenic emissions, *Atmos. Environ.*, 84, 78-87,  
743 10.1016/j.atmosenv.2013.11.032, 2014.

744 Kerminen, V. M., Chen, X. M., Vakkari, V., Petaja, T., Kulmala, M., and Bianchi, F.:  
745 Atmospheric new particle formation and growth: review of field observations, *Environ.*  
746 *Res. Lett.*, 13, Artn 103003, 10.1088/1748-9326/Aadf3c, 2018.

747 Kulmala, M., Vehkamäki, H., Petaja, T., Dal Maso, M., Lauri, A., Kerminen, V. M.,  
748 Birmili, W., and McMurry, P. H.: Formation and growth rates of ultrafine  
749 atmospheric particles: a review of observations, *J. Aer. Sci.*, 35, 143-176,  
750 10.1016/j.jaerosci.2003.10.003, 2004.

751 Langley, L., Leaitch, W. R., Lohmann, U., Shantz, N. C., and Worsnop, D. R.:  
752 Contributions from DMS and ship emissions to CCN observed over the summertime

---

753 North Pacific, *Atmos. Chem. Phys.*, 10, 1287-1314, DOI 10.5194/acp-10-1287-2010,  
754 2010.

755 Leng, C., Cheng, T., Chen, J., Zhang, R., Tao, J., Huang, G., Zha, S., Zhang, M., Fang,  
756 W., Li, X., and Li, L.: Measurements of surface cloud condensation nuclei and  
757 aerosol activity in downtown Shanghai, *Atmos. Environ.*, 69, 354-361,  
758 10.1016/j.atmosenv.2012.12.021, 2013.

759 Li, K., Zhu, Y., Gao, H., and Yao, X.: A comparative study of cloud condensation nuclei  
760 measured between non-heating and heating periods at a suburb site of Qingdao in the  
761 North China, *Atmos. Environ.*, 112, 40-53, 10.1016/j.atmosenv.2015.04.024, 2015.

762 Li, M., Liu, H., Geng, G., Hong, C., Liu, F., Song, Y., Tong, D., Zheng, B., Cui, H., Man,  
763 H., Zhang, Q., and He, K.: Anthropogenic emission inventories in China: a review,  
764 *Natl. Sci. Rev.*, 4, 834-866, 10.1093/nsr/nwx150, 2017.

765 Lin, Y. C., Chen, J. P., Ho, T. Y., and Tsai, I. C.: Atmospheric iron deposition in the  
766 northwestern Pacific Ocean and its adjacent marginal seas: The importance of coal  
767 burning, *Global. Biogeochem. Cy.*, 29, 138-159, 10.1002/2013GB004795, 2015.

768 Liu, F., Zhang, Q., A., R. J. v. d., Zheng, B., Tong, D., Yan, L., Zheng, Y., and He, K.:  
769 Recent reduction in NO<sub>x</sub> emissions over China: synthesis of satellite observations  
770 and emission inventories, *Environ. Res. Lett.*, 11, 114002, 2016.

771 Ma, N., Zhao, C. S., Tao, J. C., Wu, Z. J., Kecorius, S., Wang, Z. B., Gross, J., Liu, H.  
772 J., Bian, Y. X., Kuang, Y., Teich, M., Spindler, G., Muller, K., van Pinxteren, D.,  
773 Herrmann, H., Hu, M., and Wiedensohler, A.: Variation of CCN activity during new  
774 particle formation events in the North China Plain, *Atmos. Chem. Phys.*, 16, 8593-  
775 8607, 10.5194/acp-16-8593-2016, 2016.

776 Mochida, M., Nishita-Hara, C., Kitamori, Y., Aggarwal, S. G., Kawamura, K., Miura,  
777 K., and Takami, A.: Size-segregated measurements of cloud condensation nucleus  
778 activity and hygroscopic growth for aerosols at Cape Hedo, Japan, in spring 2008, *J.*  
779 *Geophys. Res.*, 115, 10.1029/2009jd013216, 2010.

780 Nair, V. S., Nair, J. V., Kompalli, S. K., Gogoi, M. M., and Babu, S. S.: Cloud  
781 Condensation Nuclei properties of South Asian outflow over the northern Indian  
782 Ocean during winter, *Atmos. Chem. Phys. Discuss.*, 10.5194/acp-2019-828, 2019.

---

783 O'Dowd, C., Ceburnis, D., Ovadnevaite, J., Vaishya, A., Rinaldi, M., and Facchini, M.  
784 C.: Do anthropogenic, continental or coastal aerosol sources impact on a marine  
785 aerosol signature at Mace Head?, *Atmos. Chem. Phys.*, 14, 10687-10704,  
786 10.5194/acp-14-10687-2014, 2014.

787 O'Dowd, C. D., Smith, M. H., Consterdine, I. E., and Lowe, J. A.: Marine aerosol, sea-  
788 salt, and the marine sulphur cycle: A short review, *Atmos. Environ.*, 31, 73-80, Doi  
789 10.1016/S1352-2310(96)00106-9, 1997.

790 O'Dowd, C. D., Facchini, M. C., Cavalli, F., Ceburnis, D., Mircea, M., Decesari, S.,  
791 Fuzzi, S., Yoon, Y. J., and Putaud, J. P.: Biogenically driven organic contribution to  
792 marine aerosol, *Nature*, 431, 676-680, 10.1038/nature02959, 2004.

793 Park, M., Yum, S. S., Kim, N., Cha, J. W., Shin, B., and Ryoo, S.-B.: Characterization  
794 of submicron aerosols and CCN over the Yellow Sea measured onboard the Gisang  
795 1 research vessel using the positive matrix factorization analysis method, *Atmos.*  
796 *Res.*, 214, 430-441, 10.1016/j.atmosres.2018.08.015, 2018.

797 Petters, M. D., and Kreidenweis, S. M.: A single parameter representation of hygroscopic  
798 growth and cloud condensation nucleus activity, *Atmos. Chem. Phys.*, 7, 1961-1971,  
799 DOI 10.5194/acp-7-1961-2007, 2007.

800 Phillips, B. N., Royalty, T. M., Dawson, K. W., Reed, R., Petters, M. D., and Meskhidze,  
801 N.: Hygroscopicity- and Size-Resolved Measurements of Submicron Aerosol on the  
802 East Coast of the United States, *J. Geophys. Res.-Atmos.*, 123, 1826-1839,  
803 10.1002/2017JD027702, 2018.

804 Pöschl, U., Rose, D., & Andreae, M. O. (2009). *Climatologies of Cloud-related Aerosols.*  
805 *Part 2: Particle Hygroscopicity and Cloud Condensation Nucleus Activity.* In J.  
806 Heintzenberg, & R. J. Charlson (Eds.), *Clouds in the Perturbed Climate System:*  
807 *Their Relationship to Energy Balance, Atmospheric Dynamics, and Precipitation* (pp.  
808 58-72). Cambridge: MIT Press.

809 Quinn, P. K., and Bates, T. S.: The case against climate regulation via oceanic  
810 phytoplankton sulphur emissions, *Nature*, 480, 51-56, 10.1038/nature10580, 2011.

811 Quinn, P. K., Collins, D. B., Grassian, V. H., Prather, K. A., and Bates, T. S.: Chemistry  
812 and Related Properties of Freshly Emitted Sea Spray Aerosol, *Chem. Rev.*, 115,

---

813 4383-4399, 10.1021/cr500713g, 2015.

814 Ramana, M. V., and Devi, A.: CCN concentrations and BC warming influenced by  
815 maritime ship emitted aerosol plumes over southern Bay of Bengal, *Sci. Rep.*, 6,  
816 30416, 10.1038/srep30416, 2016.

817 Rose, D., Gunthe, S. S., Mikhailov, E., Frank, G. P., Dusek, U., Andreae, M. O., and  
818 Pöschl, U.: Calibration and measurement uncertainties of a continuous-flow cloud  
819 condensation nuclei counter (DMT-CCNC): CCN activation of ammonium sulfate  
820 and sodium chloride aerosol particles in theory and experiment, *Atmos. Chem. Phys.*,  
821 8, 1153–1179, <https://doi.org/10.5194/acp-8-1153-2008>, 2008.

822 Rose, D., Nowak, A., Achtert, P., Wiedensohler, A., Hu, M., Shao, M., Zhang, Y.,  
823 Andreae, M. O., and Pöschl, U.: Cloud condensation nuclei in polluted air and  
824 biomass burning smoke near the mega-city Guangzhou, China - Part 1: Size-resolved  
825 measurements and implications for the modeling of aerosol particle hygroscopicity  
826 and CCN activity, *Atmos. Chem. Phys.*, 10, 3365-3383, DOI 10.5194/acp-10-3365-  
827 2010, 2010.

828 Rose, D., Gunthe, S. S., Su, H., Garland, R. M., Yang, H., Berghof, M., Cheng, Y. F.,  
829 Wehner, B., Achtert, P., Nowak, A., Wiedensohler, A., Takegawa, N., Kondo, Y., Hu,  
830 M., Zhang, Y., Andreae, M. O., and Pöschl, U.: Cloud condensation nuclei in polluted  
831 air and biomass burning smoke near the mega-city Guangzhou, China – Part 2: Size-  
832 resolved aerosol chemical composition, diurnal cycles, and externally mixed weakly  
833 CCN-active soot particles, *Atmos. Chem. Phys.*, 11, 2817-2836, 10.5194/acp-11-  
834 2817-2011, 2011.

835 Rosenfeld, D., Zhu, Y. N., Wang, M. H., Zheng, Y. T., Goren, T., and Yu, S. C.: Aerosol-  
836 driven droplet concentrations dominate coverage and water of oceanic low-level  
837 clouds, *Science*, 363, 10.1126/science.aav0566, 2019.

838 Royalty, T. M., Phillips, B. N., Dawson, K. W., Reed, R., Meskhidze, N., and Petters, M.  
839 D.: Aerosol Properties Observed in the Subtropical North Pacific Boundary Layer, *J.*  
840 *Geophys. Res.-Atmos.*, 122, 9990-10012, 10.1002/2017JD026897, 2017.

841 Ruehl, C. R., Chuang, P. Y., and Nenes, A.: Distinct CCN activation kinetics above the  
842 marine boundary layer along the California coast, *Geophys. Res. Lett.*, 36, L15814,

---

843 10.1029/2009gl038839, 2009.

844 Saliba, G., Chen, C. L., Lewis, S., Russell, L. M., Rivellini, L. H., Lee, A. K. Y., Quinn,  
845 P. K., Bates, T. S., Haentjens, N., Boss, E. S., Karp-Boss, L., Baetge, N., Carlson, C.  
846 A., and Behrenfeld, M. J.: Factors driving the seasonal and hourly variability of sea-  
847 spray aerosol number in the North Atlantic, *Proc. Natl. Acad. Sci. U.S.A.*, 116,  
848 20309-20314, 10.1073/pnas.1907574116, 2019.

849 Sato, Y., and Suzuki, K.: How do aerosols affect cloudiness? *Science*, 363, 580-581,  
850 10.1126/science.aaw3720, 2019.

851 Singla, V., Mukherjee, S., Safai, P. D., Meena, G. S., Dani, K. K., and Pandithurai, G.:  
852 Role of organic aerosols in CCN activation and closure over a rural background site  
853 in Western Ghats, India, *Atmos. Environ.*, 158, 148-159,  
854 10.1016/j.atmosenv.2017.03.037, 2017.

855 Song, J. W., Zhao, Y., Zhang, Y. Y., Fu, P. Q., Zheng, L. S., Yuan, Q., Wang, S., Huang,  
856 X. F., Xu, W. H., Cao, Z. X., Gromov, S., and Lai, S. C.: Influence of biomass burning  
857 on atmospheric aerosols over the western South China Sea: Insights from ions,  
858 carbonaceous fractions and stable carbon isotope ratios, *Environ. Pollut.*, 242, 1800-  
859 1809, 10.1016/j.envpol.2018.07.088, 2018.

860 Ueda, S., Miura, K., Kawata, R., Furutani, H., Uematsu, M., Omori, Y., and Tanimoto,  
861 H.: Number-size distribution of aerosol particles and new particle formation events  
862 in tropical and subtropical Pacific Oceans, *Atmos. Environ.*, 142, 324-339,  
863 10.1016/j.atmosenv.2016.07.055, 2016.

864 Wang, J., Shen, Y., Li, K., Gao, Y., Gao, H., and Yao, X.: Nucleation-mode particle pool  
865 and large increases in Ncn and Nccn observed over the northwestern Pacific Ocean  
866 in the spring of 2014, *Atmos. Chem. Phys.*, 19, 8845-8861, 10.5194/acp-19-8845-  
867 2019, 2019.

868 Wang, Z. J., Du, L. B., Li, X. X., Meng, X. Q., Chen, C., Qu, J. L., Wang, X. F., Liu, X.  
869 T., and Kabanov, V. V.: Observations of marine aerosol by a shipborne  
870 multiwavelength lidar over the Yellow Sea of China, *Proc. SPIE 9262, Lidar Remote*  
871 *Sensing for Environmental Monitoring XIV*, 926218 10.1117/12.2070297, 2014.

872 Wu, Z. J., Zheng, J., Shang, D. J., Du, Z. F., Wu, Y. S., Zeng, L. M., Wiedensohler, A.,

---

873 and Hu, M.: Particle hygroscopicity and its link to chemical composition in the urban  
874 atmosphere of Beijing, China, during summertime, *Atmos. Chem. Phys.*, 16, 1123-  
875 1138, 10.5194/acp-16-1123-2016, 2016.

876 Yamashita, K., Murakami, M., Hashimoto, A., and Tajiri, T.: CCN Ability of Asian  
877 Mineral Dust Particles and Their Effects on Cloud Droplet Formation, *J. Meteor. Soc.*  
878 Japan, 89, 581-587, 10.2151/jmsj.2011-512, 2011.

879 Yao, X. H., Lau, N. T., Fang, M., and Chan, C. K.: Real-time observation of the  
880 transformation of ultrafine atmospheric particle modes, *Aerosol. Sci. Tech.*, 39, 831-  
881 841, 10.1080/02786820500295248, 2005.

882 Yao, X. H., Lau, N. T., Chan, C. K., and Fang, M.: Size distributions and condensation  
883 growth of submicron particles in on-road vehicle plumes in Hong Kong, *Atmos.*  
884 *Environ.*, 41, 3328-3338, 10.1016/j.atmosenv.2006.12.044, 2007.

885 Yao, X. H., Choi, M. Y., Lau, N. T., Lau, A. P. S., Chan, C. K., and Fang, M.: Growth  
886 and Shrinkage of New Particles in the Atmosphere in Hong Kong, *Aerosol. Sci. Tech.*,  
887 44, 639-650, Pii 924397031,10.1080/02786826.2010.482576, 2010.

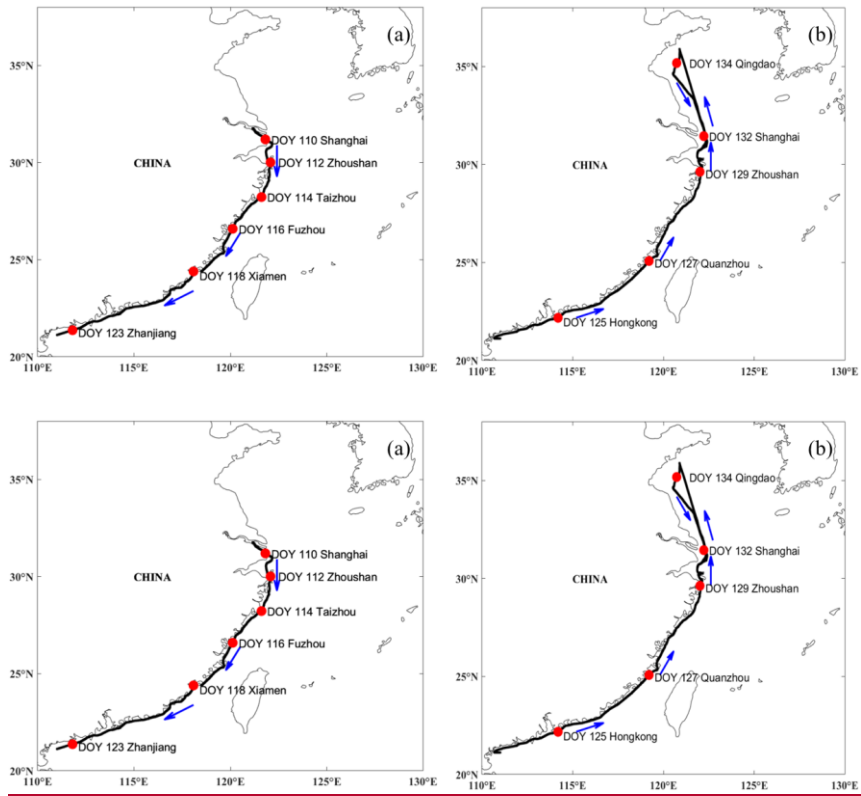
888 Yu, F., and Luo, G.: Simulation of particle size distribution with a global aerosol model:  
889 contribution of nucleation to aerosol and CCN number concentrations, *Atmos. Chem.*  
890 *Phys.*, 9, 7691-7710, DOI 10.5194/acp-9-7691-2009, 2009.

891 Zhu, Y. J., Li, K., Shen, Y. J., Gao, Y., Liu, X. H., Yu, Y., Gao, H. W., and Yao, X. H.:  
892 New particle formation in the marine atmosphere during seven cruise campaigns,  
893 *Atmos. Chem. Phys.*, 19, 89-113, 10.5194/acp-19-89-2019, 2019.

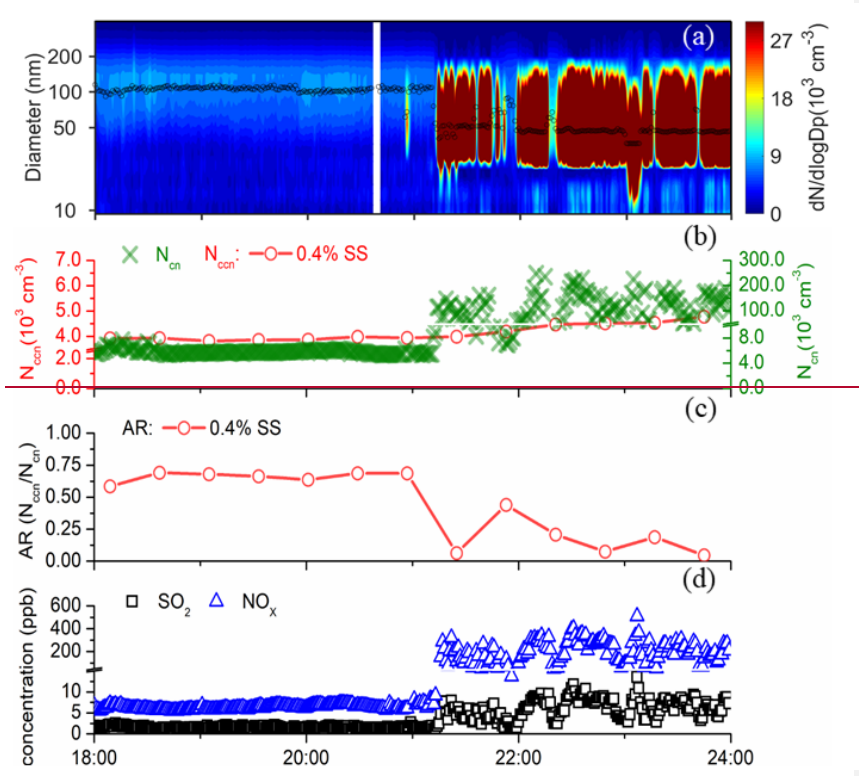
894 Zimmerman, N., Jeong, C.-H., Wang, J. M., Ramos, M., Wallace, J. S., and Evans, G.  
895 J.: A source-independent empirical correction procedure for the fast mobility and  
896 engine exhaust particle sizers, *Atmos. Environ.*, 100, 178-184,  
897 10.1016/j.atmosenv.2014.10.054, 2015.

898





**Fig 1** The ship track during the campaign of 2018, ~~and where~~ the blue arrows ~~represented~~ represent the sailing direction, with ~~the~~ southward track (a) and northward track (b).



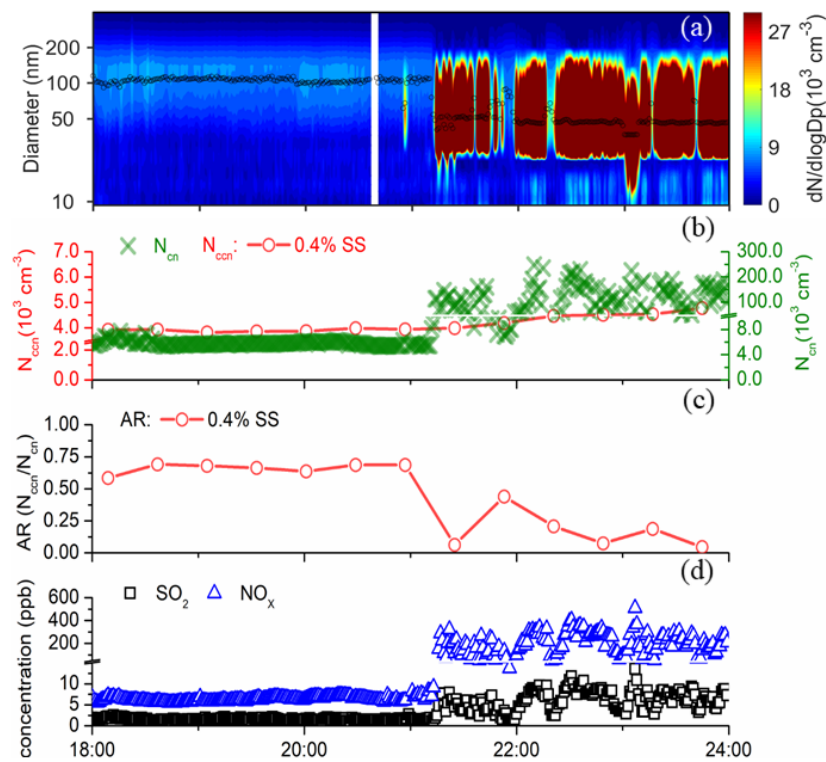


**Fig 2** Contour plot of particle number size distribution with the median mobility mode diameter shown in black hollow circles (a), time series of minutely per minute  $N_{cn}$  and half-hourly  $N_{ccn}$  at SS=0.4% (b), half-hourly AR values at SS=0.4% (c),  $\text{SO}_2$  and  $\text{NO}_x$  at nighttime on DOY 115.

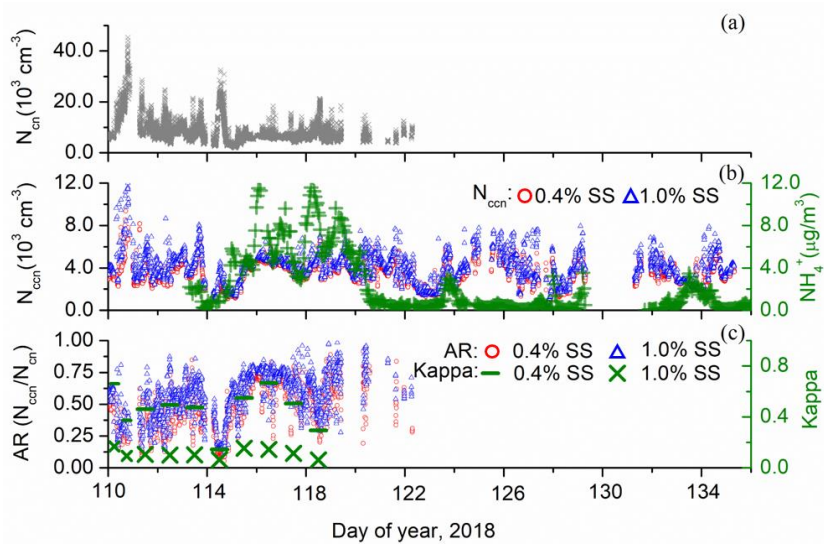


**Fig 3** Time series of minutely per minute  $N_{cn}$  from DOY 110 to 122 (a), minutely per minute  $N_{cn}$  at SS of 0.4% and 1.0% during DOY 110-135 and hourly  $\text{NH}_4^+$  during DOY 113-135 (b), and minutely per minute AR at SS of 0.4% and 1.0% during DOY 110-122 and daily *Kappa* values at SS of 0.4% and 1.0% from DOY 110 to 118 due to data availability (c). Please note that for Fig. 3c, most *Kappa* values were based on a daily scale, except on DOY 110, during which two *Kappa* values were calculated from 00:00-06:00 and 08:00-21:00, respectively.

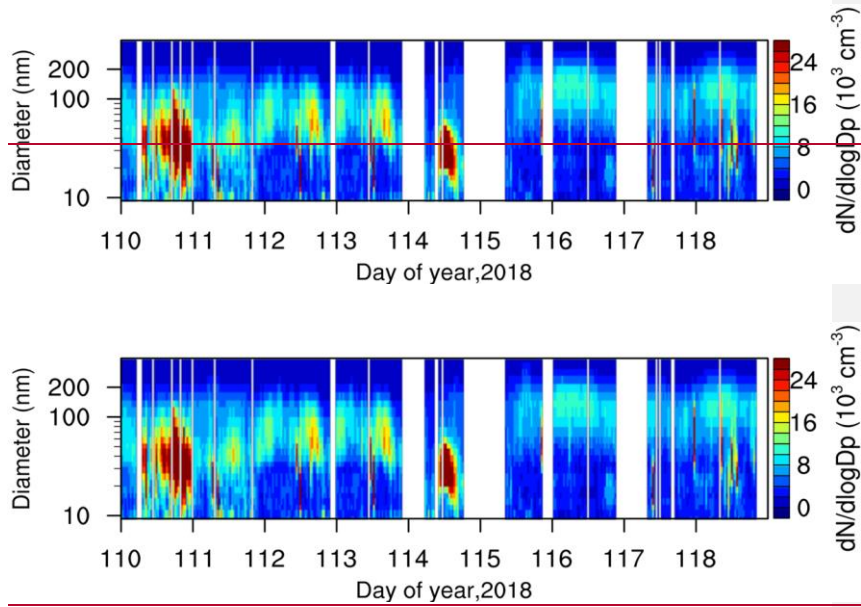


**Fig 4** Contour plot of particle number size distribution on DOY 110-118 with ship self-~~ship~~ emission signals removed.-

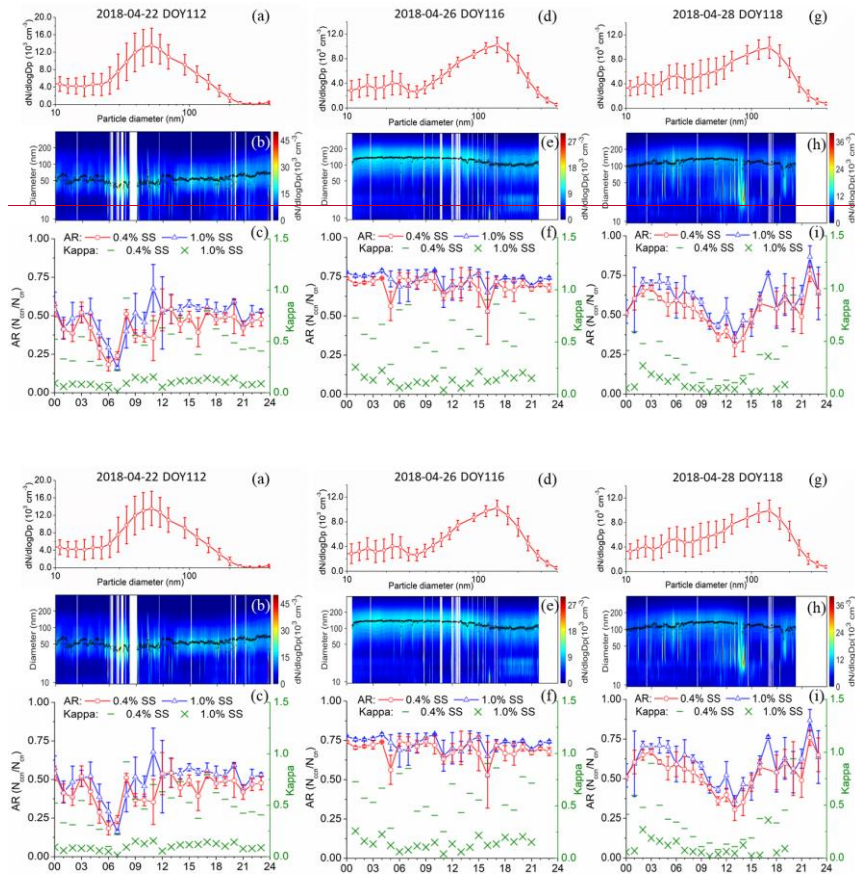
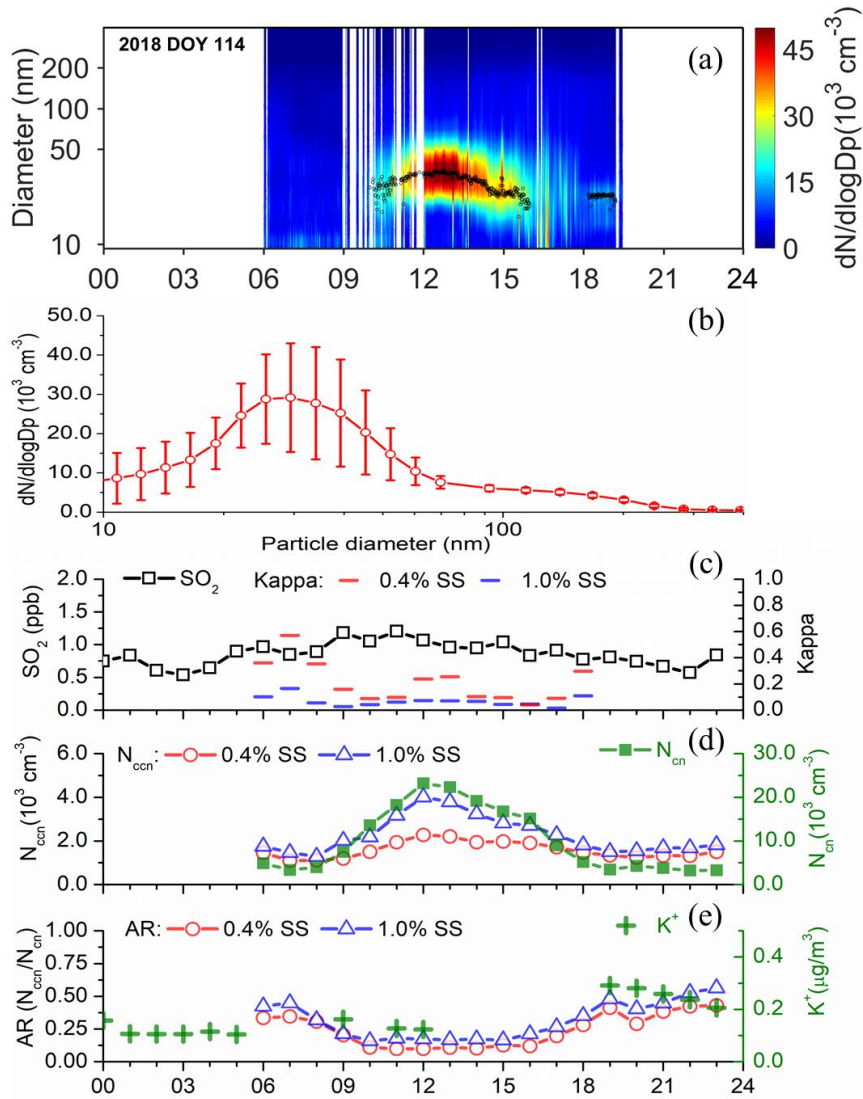
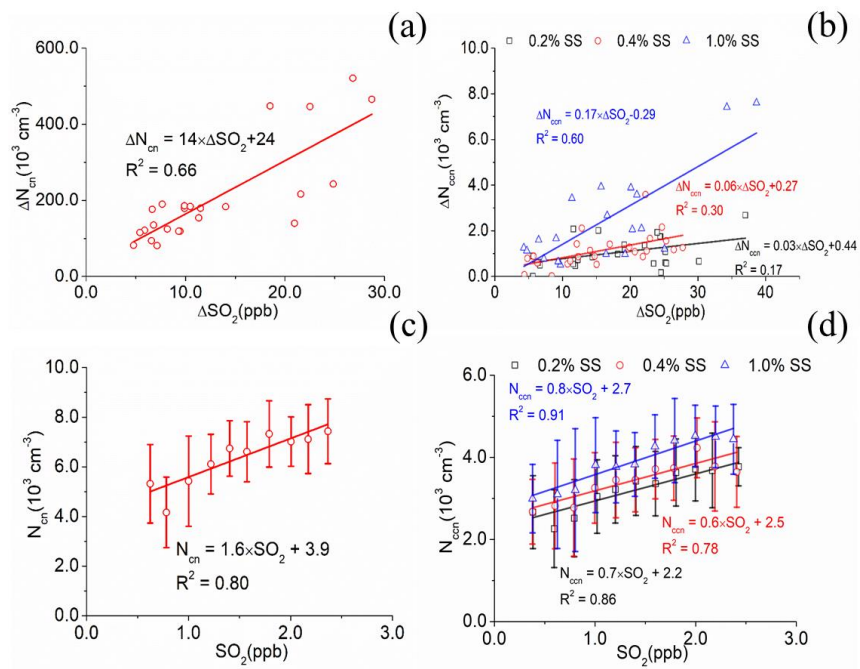


Fig 5 Daily average (top row) and contour plot (middle row) of particle number size distributions, and time series of hourly averaged AR at SS of 0.4% and 1.0% and Kappa value on DOY112, DOY116 DOY 112, DOY 116 and DOY118 DOY 118. The bars represent the standard deviation, with the mean indicated by the hollow circles. –



**Fig 6** Contour plot of particle number size distributions for the day of DOY 114 2018 (a), the size distributions of the particle number concentration during 10:00 -18:00 LT DOY 114 2018 (b), time series of hourly averaged  $\text{SO}_2$  and  $Kappa$  values at SS of 0.4% and 1.0% (c),  $N_{ccn}$  at SS of 0.4% and 1.0% (d), and AR values at SS of 0.4% and 1.0% and  $K^+$  (e) for the day of DOY 114 2018.



**Fig 7** CorrelationsRelationship of hourly averaged  $N_{cn}$  and  $N_{ccn}$  with  $SO_2$  at SS of 0.2%, 0.4% and 1.0%. For Fig. 7a,b,  $\Delta N_{cn}$ ,  $\Delta N_{ccn}$  and  $\Delta SO_2$  reflects reflect the impact from of the ship self-ship-emission after the removal of the ambient concentration. For Fig. 7c, d, each bar indicates the standard deviation with the mean value marked as the hollow circles (or triangles, squares), and the interval of  $SO_2$  is 0.2 ppb for each bar.



**Table 1.**  $N_{cn}$  and  $N_{ccn}$ , AR and  $SO_2$  mixing ratios on DOY 110-135, 2018, over ~~China~~ marginal seas in China. Please note that  $N_{cn}$  and AR are from 110-122, 2018.

| <del>Variables</del> <u>Variable</u>  | Supersaturation<br>(SS) | <del>Ranges</del> <u>Range</u> | Mean $\pm$ standard<br>deviation |
|---------------------------------------|-------------------------|--------------------------------|----------------------------------|
| $N_{cn}$ ( $\times 10^3$ $cm^{-3}$ )  |                         | 2.0-45                         | 8.1 $\pm$ 4.4                    |
|                                       | SS=0.2%                 | 0.4-8.8                        | 3.2 $\pm$ 1.1                    |
|                                       | SS=0.4%                 | 0.5-9.4                        | 3.4 $\pm$ 1.1                    |
| $N_{ccn}$ ( $\times 10^3$ $cm^{-3}$ ) | SS=0.6%                 | 0.5-8.6                        | 3.6 $\pm$ 1.2                    |
|                                       | SS=0.8%                 | 0.5-11                         | 3.8 $\pm$ 1.2                    |
|                                       | SS=1.0%                 | 0.6-12                         | 3.9 $\pm$ 1.4                    |
|                                       | SS=0.2%                 | 0.06-0.89                      | 0.49 $\pm$ 0.17                  |
|                                       | SS=0.4%                 | 0.06-0.92                      | 0.51 $\pm$ 0.17                  |
| AR                                    | SS=0.6%                 | 0.10-0.94                      | 0.54 $\pm$ 0.17                  |
|                                       | SS=0.8%                 | 0.08-0.95                      | 0.56 $\pm$ 0.17                  |
|                                       | SS=1.0%                 | 0.11-0.98                      | 0.57 $\pm$ 0.17                  |
| $SO_2$ (ppb)                          |                         | 0.25-9.7                       | 1.7 $\pm$ 1.1                    |

Formatted: Font: Symbol